

AFML-TR-68-257

AD 626275

**THE EFFECTS OF BUMPER MATERIAL PROPERTIES
ON THE OPERATION OF SPACED
HYPERVELOCITY PARTICLE SHIELDS**

H. F. Swift

University of Dayton

A. K. Hopkins

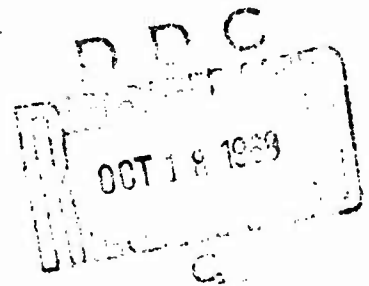
Air Force Materials Laboratory

TECHNICAL REPORT AFML-TR-68-257

September 1968

**This document has been approved for public release
and sale; its distribution is unlimited.**

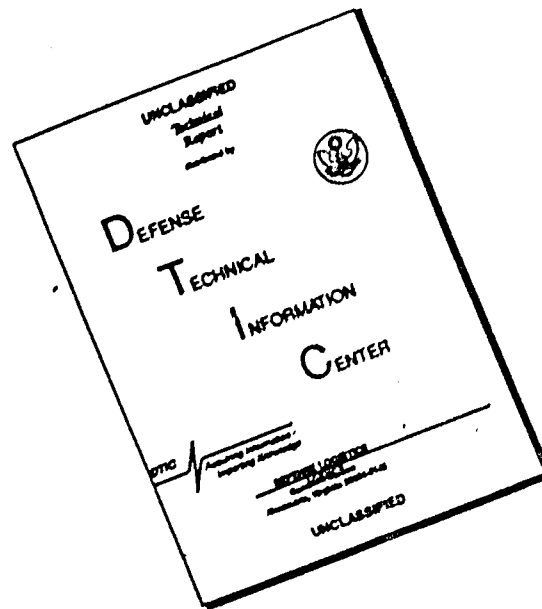
**Air Force Materials Laboratory
Air Force Systems Command
Wright-Patterson Air Force Base, Ohio**



Reproduced by the
CLEARINGHOUSE
for Federal Scientific & Technical
Information Springfield Va. 22154

52

DISCLAIMER NOTICE



THIS DOCUMENT IS BEST QUALITY AVAILABLE. THE COPY FURNISHED TO DTIC CONTAINED A SIGNIFICANT NUMBER OF PAGES WHICH DO NOT REPRODUCE LEGIBLY.

NOTICES

When Government drawings, specifications, or other data are used for any purpose other than in connection with a definitely related Government procurement operation, the United States Government thereby incurs no responsibility nor any obligation whatsoever; and the fact that the Government may have formulated, furnished, or in any way supplied the said drawings, specifications, or other data, is not to be regarded by implication or otherwise as in any manner licensing the holder or any other person or corporation, or conveying any rights or permission to manufacture, use, or sell any patented invention that may in any way be related thereto.

ACQUISITION NO.		
CPSTI	WHITE SECTION <input checked="" type="checkbox"/>	
DDC	BLUE SECTION <input type="checkbox"/>	
UNANNOUNCED	<input type="checkbox"/>	
JUSTIFICATION		
BY		
DISTRIBUTION/AVAILABILITY CODES		
DIST.	AVAIL. CODE	SPECIAL
1		

Copies of this report should not be returned unless return is required by security considerations, contractual obligations, or notice on a specific document.

AFML-TR-68-257

THE EFFECTS OF BUMPER MATERIAL PROPERTIES
ON THE OPERATION OF SPACED
HYPERVELOCITY PARTICLE SHIELDS

H. F. Swift
University of Dayton

A. K. Hopkins
Air Force Materials Laboratory

This document has been approved for public release
and sale; its distribution is unlimited

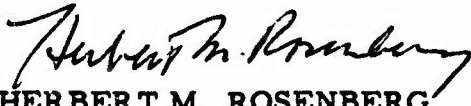
FOREWORD

This report covers research performed on the AFML light-gas gun facility. Part of the reporting effort was pursued by AFML personnel and the remainder was conducted by the University of Dayton Research Institute, Dayton, Ohio under Air Force Contract F33615-68-C-1138, Project 7360, Chemistry and Physics of Materials, Task 736006, Hypervelocity Impact Studies. Experimental work covered in this report was completed during July 1968. The portion of the research performed by the University of Dayton Research Institute was administered by Mr. Alan K. Hopkins, Project Engineer, AFML.

The authors gratefully acknowledge the support of the facility operations group under the direction of Mr. Lewis Shiverdecker.

The manuscript was released by the authors in August 1968 for publication with a University of Dayton report number UDRI-TR-68-30.

This technical report has been reviewed and is approved.


HERBERT M. ROSENBERG
Chief, Exploratory Studies Branch
Materials Physics Division
Air Force Materials Laboratory

ABSTRACT

An experimental study has been conducted to evaluate the importance of bumper materials selection upon the performance of two-component hypervelocity impact bumper shields. Several bumper materials were found that were equally effective on a mass per unit area basis. Bumper material effectiveness dropped rapidly with bumper material density when this density was below 2 gm/cc. Optimum bumper thicknesses exist for minimizing total shield weight for all bumper materials investigated. All of the data obtained in this study can be explained by an analysis of the states of the impacting pellet and bumper material within the debris cloud projected behind impacted bumpers. The most important parameter controlling shield operation is the state of the pellet material in the debris cloud.

TABLE OF CONTENTS

	<u>Page</u>
INTRODUCTION	i
BACKGROUND	2
EXPERIMENTAL DESIGN AND RESULTS	4
Constant Bumper Areal Density Study	5
Effects of Bumper Material Physical Properties	8
Effects of Optimizing Bumper Thickness Upon Particle Shield Operation	13
DISCUSSION	16
Operational Hypothesis and Related Observations	16
Shock Wave Heating Evaluation	18
CONCLUSIONS	21
REFERENCES.	24
APPENDIX I	26
APPENDIX II	37

LIST OF ILLUSTRATIONS

<u>Figure No.</u>		<u>Page</u>
1	Data Plot for Constant Bumper Areal Density Study . . .	7
2	Witness Plates Behind Bumpers Made From Materials Obeying Constant Areal Density Relationships	9
3	Witness Plates Behind Bumpers Whose Materials Were Vaporized by Pellet Impacts	10
4	Witness Plates Behind Bumpers Whose Materials Were Fragmented by Pellet Impacts	10
5	Witness Plates Behind Bumpers Whose Material Densities Are Below 2 gm/cc.	11
6	Witness Plate and Total Shield Area Density vs. Bumper Areal Density	14
7	Total Shield Area Density vs. Bumper Areal Density for Five Representative Bumper Materials.	15
8	Witness Plate Areal Density vs. Bumper Areal Density for Five Representative Bumper Materials . . .	15
9	Peak Shock Impact Pressure Generated by Aluminum Pellet Impact vs. Bumper Material Density	19
10	Temperature vs. Internal Energy of an Arbitrary Crystalline Material Showing Melting and Vaporization	21
11	Data Plot for Constant Bumper Areal Density Study Showing States of Bumper and Pellet Materials in the Debris Clouds	22
12	Areal Densities of Witness Plates and Complete Shield vs. Bumper Areal Density for Paraffin Bumpers	32

List of Illustrations (Continued)

<u>Figure No.</u>		<u>Page</u>
13	Areal Densities of Witness Plates and Complete Shield vs. Bumper Areal Density for Magnesium Bumpers	33
14	Areal Densities of Witness Plates and Complete Shield vs. Bumper Areal Density for Teflon Bumpers	34
15	Areal Densities of Witness Plates and Complete Shield vs. Bumper Areal Density for Steel Bumpers	35
16	Areal Densities of Witness Plates and Complete Shield vs. Bumper Areal Density for Cadmium Bumpers	36
17	One-Dimensional Shock Impact Pressure of Aluminum vs. Aluminum Particle Velocity.	38
18	Shock Pressure-Particle Velocity Plots for the Bumper Materials Used in This Study	40
19	Shock Pressure-Specific Volume Plot for an Arbitrary Material Showing Hugoniot, Release Adiabats, Rayleigh Line, Energy Inserted During Shock Compression and Energy Released by Material Expansion	41

LIST OF TABLES

<u>Table No.</u>		<u>Page</u>
1	Parameters of the Bumper Areal Density Experiment . .	5
2	Resume of Data From Bumper Materials Properties Study.	6
3	Effects of Bumper Material Microstructure on Overall Shield Effectiveness	12
4	Shock Heating Data for Some Materials Used for the Bumper Materials Effects Study	20
5	Firing Data for All Gas Gun Rounds Used for the Bumper Materials Effects Study.	27
6	Shock Pressures Induced in Bumper Materials When Impacted by Aluminum Pellets Traveling at 7.0 km/sec.	42

THE EFFECTS OF BUMPER MATERIAL PROPERTIES ON THE OPERATION OF SPACED HYPERVELOCITY PARTICLE SHIELDS

I. INTRODUCTION

Large space vehicles committed to long duration missions are subject to potentially disastrous encounters with meteoroids. Protection against this hazard must be provided to assure adequate mission reliability.

The "bumper shield" concept originally proposed by Whipple⁽¹⁾ remains, after considerable evaluation, the most promising technique for providing the required protection against particle impacts. The protected component (such as the vehicle hull) is shielded from direct impacts by interposing a relatively thin continuous sheet of material (bumper) some distance in front of the protected component to intercept incoming particles. Incoming particles impact the bumper and are disintegrated, and the protected component must withstand encounters with relatively diffuse debris clouds from the bumper-particle impacts. The resultant reduction of spacial impact intensity on the protected component allows it to be lightened enough to more than offset the weight of the bumper without sacrificing overall impact resistance. Equivalent impact resistance has been demonstrated for bumpered structures weighing as little as 20% of corresponding single plate shield⁽²⁾.

Many studies of both general bumper shield structures and specific structures proposed for particular vehicles have been carried out^(2, 3, 4). In all cases, the impact velocities used for the studies are significantly below those anticipated for encounters with macroparticles in space. The required velocity extrapolations between laboratory tests and space environment are hazardous unless the phenomena controlling particle shield operation are well understood. This report covers one phase of an AFML effort to evaluate bumpered particle shield effectiveness and the phenomena controlling shield operation. The effects of bumper materials properties on overall shield effectiveness have been investigated. The results from this study help to delineate the requirements for bumper materials and configurations needed to optimize shield

effectiveness and can be used to elucidate some processes controlling the operation of bumpered shields.

II. BACKGROUND

The following qualitative description of impacts between hypervelocity pellets and thin plates has been widely accepted by workers in the hypervelocity impact field. Upon impact, strong compressive shock waves propagate forward and outward into the plate and rearward into the oncoming pellet. These waves are attenuated by pressure release waves that propagate inward from all free surfaces encountered by the compressive waves. The compressive and release waves establish a material flow field that controls the ultimate disposition of both the pellet and plate material. The bulk of this material is projected behind the plate in an expanding bubble while almost all the remainder is projected in front of the plate along a conical surface centered around the original pellet trajectory. A small amount of impulse that is trapped in the plate projects laterally outward from the impact point and is responsible for forming the final hole in the plate.

The direction, speed, spacial density, and physical state of the material projected behind the plate are determining factors in establishing the damage potential of debris clouds. Two approaches are currently available to vehicle designers to predict this damage potential. Rolsten, et al.⁽⁵⁾ noted that, over a wide range of material properties, equal bumper areal densities produced debris clouds with approximately equal damage potential (i. e. thick bumpers of low density material behave in a similar manner to proportionately thinner bumpers made from higher density material). Rolsten examined materials whose densities ranged from magnesium-lithium alloy ($\rho = 1.35 \text{ gm/cc}$) to steel ($\rho = 7.8 \text{ gm/cc}$). This concept was later verified by using gold bumpers ($\rho = 19.24 \text{ gm/cc}$)⁽⁶⁾. Riney and Heyda came to a similar conclusions from a purely theoretical study of impacts between aluminum cylinders and thin plates at 15 km/sec ⁽⁷⁾. They computed the ratio between the debris cloud impulse directed along the original pellet trajectory and the outward directed impulse perpendicular to the pellet trajectory for several bumpers subjected to identical hypervelocity impacts. These ratios correlated with the total areal density of the bumper configurations only. Riney and Heyda reasoned that these impulse ratios determined the effectiveness of bumpers for diffusing the pellet impulse and, hence, the overall bumper effectiveness.

It is of interest to note that total mass of debris clouds falls monotonically with increasing density of bumper material when equal bumper areal densities are maintained. Several investigators have noted

that the hole diameters in thin plates impacted by hypervelocity pellets decrease rapidly with decreasing plate thickness^(3,8,9). For example, Maiden and McMillan developed the following empirical expression for determining hole diameters that predicts a 2/3 power relationship between plate thickness and hole diameter.

$$\frac{D}{d_0} = 2.4 \left(\frac{v}{c} \right) \left(\frac{t}{d_0} \right)^{2/3} + .9 \quad (1)$$

D = hole diameter

d₀ = projectile diameter

t = plate thickness

v = pellet velocity

c = sound speed in the plate

Carson and Swift disagree with the above expression in detail but agree with the general trends⁽⁹⁾.

Systematic decreases in hole diameters lead to similar decreases in the material available to the debris cloud since: the cloud is made up of the pellet material plus material removed from the bumper; and the available bumper material is a function of hole diameter only. Thus, debris clouds generated behind high-density bumpers contain less material and yet are equally destructive. For this to be so, some mechanism must be operating to counteract the effects of changes in total debris cloud mass with changes in bumper density.

Maiden and McMillan reported significant differences in bumper effectiveness that were correlated with the fusion and sublimation energies of the pellet and bumper materials⁽³⁾. They follow an earlier argument presented by Bjork, et al.⁽¹⁰⁾ that the primary compressive waves generated by a hypervelocity impact are sufficiently intense to significantly increase the entropy of the material through which they propagate. The unloading waves that return the material to zero pressure are nearly isentropic regardless of their pressure span. Thus, entropy is trapped in materials subjected to intense shock compression. The trapped entropy appears as internal energy of materials after they have returned to zero pressure. If the increase in internal energy is greater than that required to heat the material to the melting point plus the material fusion energy the material returns to zero pressure in the liquid state. The material returns to zero pressure as vapor if the

internal energy increase exceeds the material sublimation energy. Maiden and McMillan discovered that impact debris clouds of solid particles are considerably more destructive than those made up from liquid droplets and that both are more destructive than gaseous debris clouds⁽³⁾. Thus, the thermodynamic properties of pellet and bumper materials strongly affect the operation of bumper particle shields. These results have been verified by Zwarts⁽⁴⁾ and Carey⁽¹¹⁾. This line of argument leads to the prediction that bumpers with equal areal densities will not be equally effective if they create debris clouds whose materials are in different physical states. Thus, the two approaches to determining bumper effectiveness appear to contradict each other at least in this regard.

The ranges of applicability of these two approaches for predicting bumper shield effectiveness (i. e. constant-area density rule or thermodynamic considerations) and their apparent contradictions must be resolved before reliable space vehicle shields can be designed. Current laboratory accelerators can achieve pellet velocities required for generating either solid or liquid debris clouds when realistic pellet and bumper structural materials are tested but cannot generate vaporous clouds with these materials. Vaporous clouds can be generated with laboratory accelerators by employing low sublimation-energy materials such as plastics, cadmium, tin, lead, etc. for the pellets and bumpers. To date, the tests carried out to investigate debris cloud phase variation have employed only identical pellet and plate materials^(4, 6, 11). Thus, no experimental data capable of separating the independent effects of melting or vaporizing the pellets and the bumpers were available prior to this study.

III. EXPERIMENTAL DESIGN AND RESULTS

The overall purpose of the experimental sequence for this study was to compare the relative effectiveness of bumpers made from a wide variety of materials. This effectiveness was established by determining the thickness of 6061-T6 aluminum plates required to just prevent perforations by debris clouds when placed 5.08 cm behind impacted bumpers. All other impact and target parameters were held relatively constant. The resistance limit of the rear plate (ballistic limit) was defined for this study as the minimum plate thickness that would maintain a gas seal after impact. This rear plate thickness is considered a quantitative measure of the relative destructive potential the debris clouds generated for this study.

Constant Bumper Areal Density Study

One series of firings was carried out to determine the accuracy and range of validity of the constant-areal-density rule. The relative effectiveness of 16 bumper materials where all bumpers had near identical areal densities was determined. The bumper thicknesses were adjusted to achieve a predetermined bumper mass per unit of presented area (i. e. bumpers made from low density materials were proportionately thicker than higher density ones). The areal density chosen for this series was that of optimum-thickness 6061-T6 aluminum bumpers established during a previous study⁽²⁾. The other firing parameters are presented in Table I. Note that pellet velocities varied over an extended range. Earlier studies showed (and this study has verified) that rear plate ballistic limit thicknesses are highly insensitive to pellet velocities in the velocity regime used for these experiments. No anomalous results caused by pellet velocity variations within the range of this investigation were detected during either this study or other similar ones conducted earlier at AFML⁽²⁾.

TABLE I

Parameters of the Bumper Areal Density Experiment

Pellet

3.18 mm dia 2017 aluminum spheres	mass = 45.9 to 47.1 milligrams velocity = 6.2 to 7.4 km/sec
--------------------------------------	--

Rear Plate

6061-T6 aluminum rolled plate	thickness = variable
----------------------------------	----------------------

Bumper

material = variable material density = 0.84-16.64 gm/cc areal density = .210-.249 gm/cm ²
--

Bumper-Target Spacing = 5.08 cm

The results from these experiments are presented in Table II and Figure 1. A complete listing of data from all the firings used to generate these data is presented in Appendix I. The double values presented in the "Target" and "Total" columns of Table II represent the ballistic limit resolution achieved for each case considered. The plot of rear plate thickness and areal density vs. bumper material

TABLE II

Resume of Data From Bumper Materials Properties Study

Material	BUMPER			TARGET		TOTAL SHIELD	CLOUD STATE (Appendix II and Table IV)	
	Density gm/cc	Thickness cm	Microstructure	Thickness cm	Mass/Area gm/cm ²		Bumper	Pellet
Paraffin	0.84	0.254	Amorphous	.295-.307	.786-.820	.996-1.030	Gas*	Solid
Polyethylene	0.92	0.236	Polymer	.279-.292	.745-.779	.963-.997	Gas*	Solid
Ice	0.92	0.246	Crystalline	.279-.292	.745-.779	.972-1.006	Gas*	Solid
Water	1.00	0.234	Amorphous	.257-.279	.686-.745	.920-.979	Gas*	Solid
Mg-Li (alloy)	1.37	0.157	Crystalline	.218-.229	.582-.611	.797-.826	Liquid*	Solid
Magnesium	1.76	0.127	Crystalline	.160-.203	.427-.542	.650-.766	Liquid	Solid
Glass (crown)	2.19	0.104	Amorphous	.130-.142	.347-.379	.575-.607	Liquid*	Liquid
Teflon	2.31	0.099	Polymer	.130-.145	.345-.386	.575-.616	Liquid	Liquid
Aluminum (6061)	2.67	0.084	Crystalline	.140-.145	.373-.386	.596-.609	Liquid	Liquid
Titanium	4.46	0.051	Crystalline	.127-.140	.339-.374	.566-.601	Liquid	Liquid
Steel (1020)	7.65	0.030	Crystalline	.140-.152	.373-.406	.609-.643	Liquid	Liquid
Cadmium	8.26	0.028	Crystalline	.114-.127	.305-.338	.535-.568	Gas	Liquid
Nickel	8.73	0.028	Crystalline	.173-.191	.462-.510	.710-.758	Solid	Liquid
Copper	8.78	0.028	Crystalline	.127-.140	.339-.374	.588-.623	Liquid	Liquid
Lead	10.82	0.020	Crystalline	.102-.114	.272-.304	.498-.520	Gas	Liquid
Tantalum	16.64	0.013	Crystalline	.173-.191	.460-.508	.670-.718	Solid*	Liquid

* Postulated from character of debris on witness plate or target.

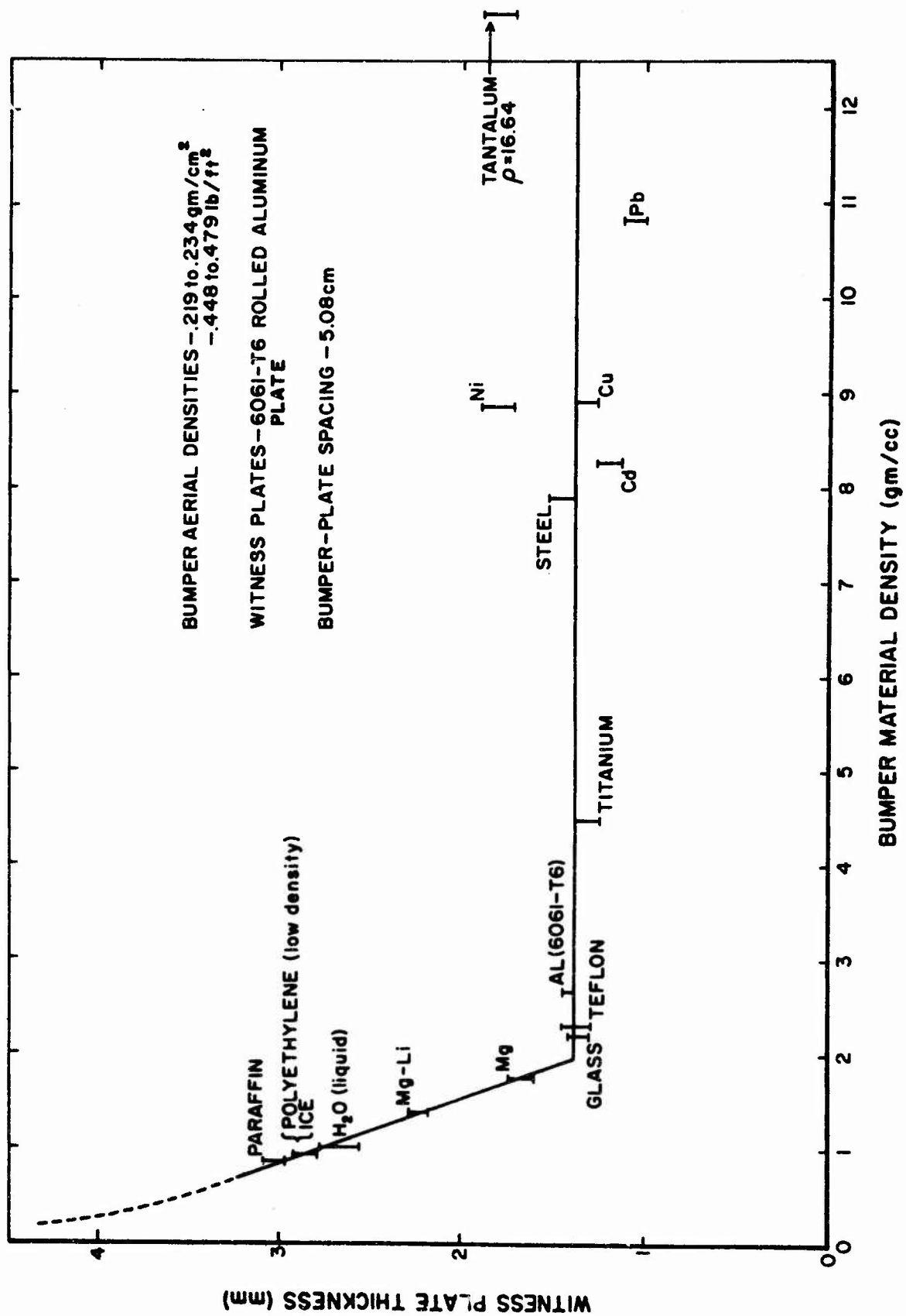
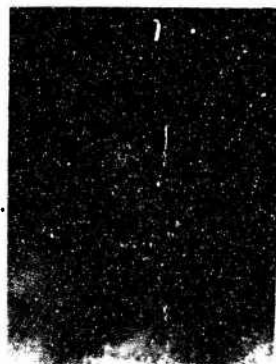


Figure 1. Data Plot for Constant Bumper Areal Density Study

density presented in Figure 1 illustrates that several bumper materials whose material density is greater than 2 gm/cc adhere to the constant-areal-density rule but that there are many exceptions. Figure 2 presents photographs of the plates mounted behind bumpers that follow the constant-areal-density rule. Data from some bumper materials fall below the constant-areal-density line (Cd, Pb) [see Figure 3] and some fall above it (Ni, Ta) [see Figure 4]. The most striking feature of Figure 1 is the extreme excursion from the constant-areal-density line that occurs when bumpers whose material density is below 2 gm/cc were examined. Photographs of the rear plates mounted behind these bumpers are presented in Figure 5. A rapidly rising linear function appears to fit the rear plate areal density vs. bumper material density plot over the density range observed. This function must steepen for bumper material densities below those examined since the rear plate thickness for zero density bumpers (i.e. no bumper at all) has been determined earlier to be 11.23-11.35 mm⁽²⁾. Extrapolation of the current curve yields a value of 3.95 mm. This sharp reduction in bumper effectiveness with decreasing material density is of considerable importance to the design of practical particle shields for space vehicles.

Effects of Bumper Material Physical Properties

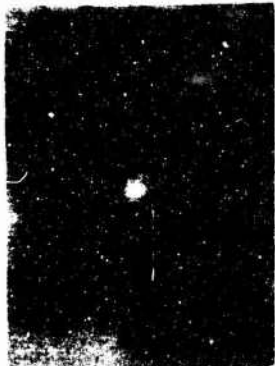
The other physical properties of bumper materials besides material density and thermodynamic variables should have little or no effect upon the formation of the high-energy-content segments of debris clouds caused by hypervelocity impacts. Relatively large fragments propelled rearward from impacted bumpers at relatively late times in the process may contribute to the overall debris-cloud damage. The formation and launching of these fragments are affected by the strength and high strain-rate behavior of the bumper material. Thus, it is conceivable that variations in the physical properties of the materials will control bumper effectiveness. Both the qualitative and quantitative aspects of the high strain-rate behavior of materials vary widely and these variations are especially marked between materials with different microstructures (i.e. crystalline, polymer, amorphous). Two groups of materials representing the principle microstructure groups and having as nearly identical densities as feasible were chosen for constant-bumper-areal-density evaluations. The materials in group I have densities above 2 gm/cc and should follow the constant-areal-density rule while those in group II have densities well below 2 gm/cc placing them in the region where bumper material density affects bumper performance. The results of the bumper microstructure evaluation are presented in Figure 1 and Table III. No effect of material microstructure is observable in these data. The materials in group I obey the constant-areal-density rule within the resolution of the data. The



GLASS
 $\rho = 2.19 \text{ gm/cc}$



TEFLON
 $\rho = 2.31 \text{ gm/cc}$



ALUMINUM
 $\rho = 2.67 \text{ gm/cc}$



TITANIUM
 $\rho = 4.46 \text{ gm/cc}$

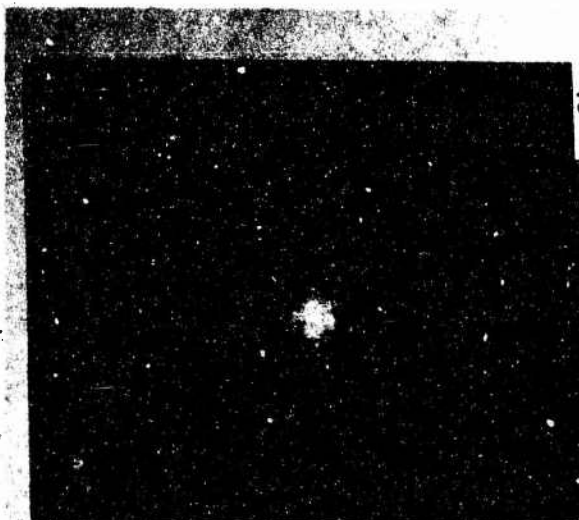


IRON
 $\rho = 7.65 \text{ gm/cc}$

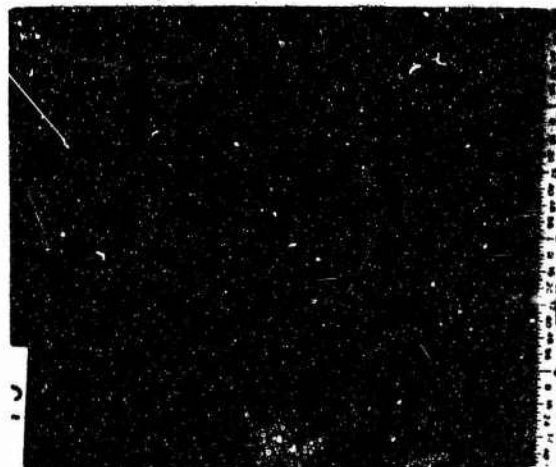


COPPER
 $\rho = 8.78 \text{ gm/cc}$

Figure 2. Witness Plates Behind Bumpers Obeying
Constant Areal Density Relationships.

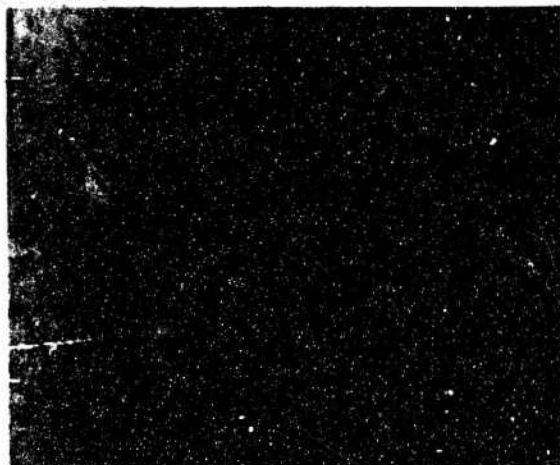


CADMIUM
 $\rho = 8.26 \text{ gm/cc}$

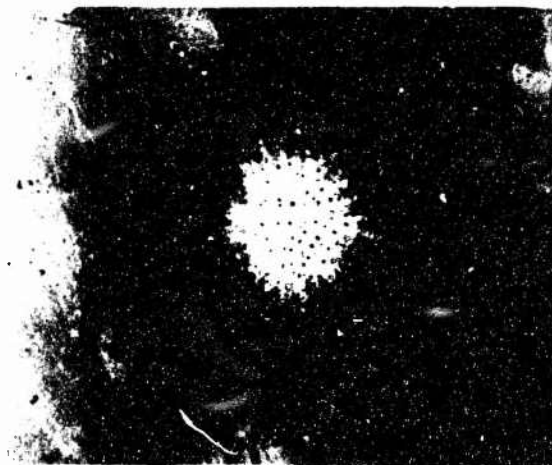


LEAD
 $\rho = 10.82 \text{ gm/cc}$

Figure 3. Witness Plates Behind Bumpers Whose Materials Were Vaporized by Pellet Impacts



NICKEL
 $\rho = 8.73 \text{ gm/cc}$



TANTALUM
 $\rho = 16.64 \text{ gm/cc}$

Figure 4. Witness Plates Behind Bumpers Whose Materials Were Fragmented by Pellet Impacts

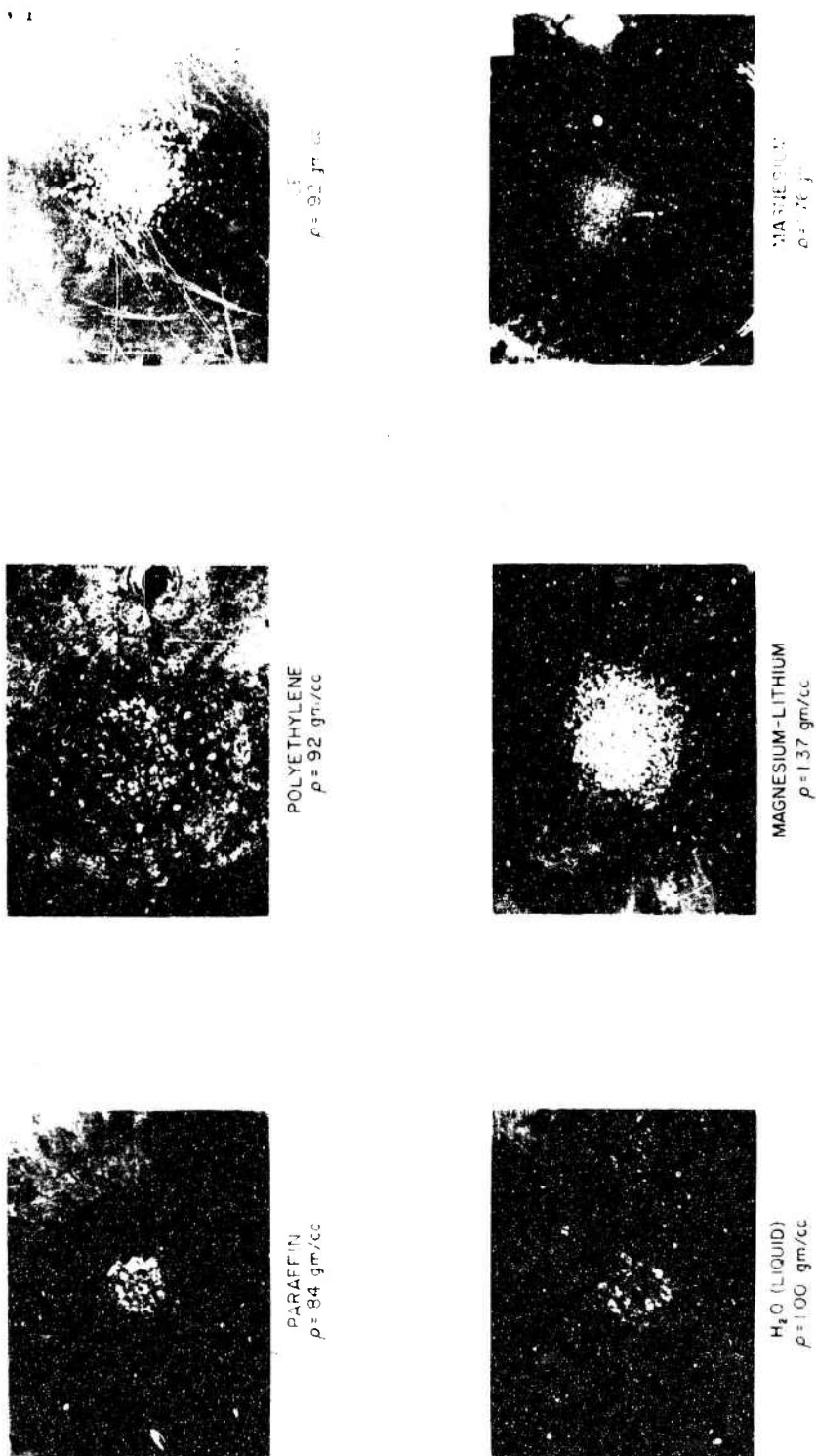


Figure 5. Witness Plates Behind Bumpers Whose Material Densities are Below 2 gm/cc

TABLE III

Effects of Bumper Material Microstructure on Overall Shield Effectiveness

Material	Density gm/cc	Microstructure	Bumper Effectiveness	
			Rear Plate Thickness cm	*Shield Areal/Density gm/cm ²
6061-Al Teflon Crown Glass	2.67 2.31 2.19	Group I ($\rho = 2.2-2.7$ gm/cc)		
		Crystalline	.140-.145	.595-.609
		Polymer	.130-.145	.575-.616
Ice Polyethylene Water	.92 .92 1.00	Group II ($\rho = .92-1.00$ gm/cc)		
		Crystalline	.279-.292	.972-1.006
		Polymer	.279-.292	.963-.997
		Amorphous	.257-.279	.920-.979

*Shield is considered as the bumper plus the rear target.

shifts in material effectiveness observed among the materials in group II can be correlated with the overall dependence of bumper effectiveness upon material density as shown in Figure 1.

Effects of Optimizing Bumper Thickness Upon Particle Shield Operation

Several investigations of spaced particle shields have indicated that optimum bumper thicknesses exist for particular impact situations^(2, 3, 5). Basically, extremely thin bumpers fail to completely disrupt incoming pellets or to spread the impact debris over a sufficient area for component protection. Excessive bumper thickness directly reduces overall shield weight effectiveness, and may increase the damage potential of the debris clouds by increasing the average size of the projected fragments. Some bumper materials used in the constant-areal-density study may appear less effective than they actually could be since bumper thicknesses which were not optimum were used. Therefore, the effects of bumper optimization must be investigated before definite conclusions regarding overall shield effectiveness can be drawn.

Two criteria are possible for defining optimum bumper thicknesses. The first is to minimize the total shield areal density, which has obvious engineering significance. The second, and closely related criterion is that of optimizing the bumper thickness to provide a debris cloud of minimal damage potential as defined by the rear plate ballistic limit thickness.

A firing sequence was carried out where the ballistic limit thickness of rear plates was determined for each of several thicknesses of several different bumper materials employed in the constant-areal-density study. Figure 6 is a plot of rear plate areal density and total areal density vs. bumper plate thickness of 6061-T6 aluminum bumpers. Note that the optimum bumper thickness required to produce a minimum total shield areal density is significantly less than that required to produce a debris cloud with minimum destructive potential. This shift between the two optimization criteria arises because rear target areal density is reduced to a lesser degree by generating a minimally destructive debris cloud than is expended in increasing bumper thickness to produce minimally destructive clouds.

Five materials, paraffin, magnesium, 6061-T6 aluminum, steel and cadmium were chosen as representative of the materials considered in the constant-areal-density study for the bumper thickness investigation. Paraffin and magnesium have low enough material densities to place them in the density dependent region of the bumper

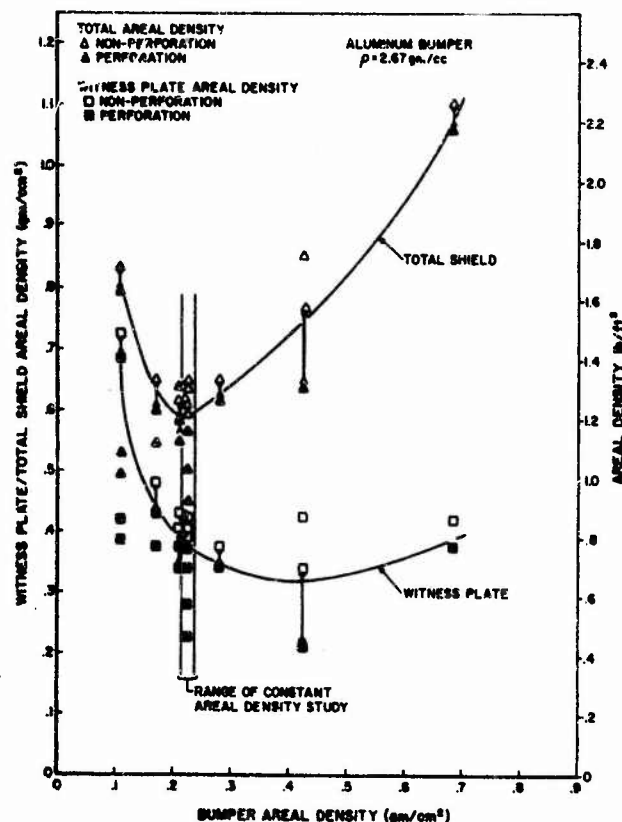


Figure 6. Witness Plate and Total Shield Areal Density vs. Bumper Areal Density

effectiveness plot (Figure 1). Aluminum and steel are materials that obey the constant-areal-density rule and cadmium is a material which fails to obey this rule.

The overall results of the bumper thickness investigation appear in Figures 7 and 8. Detailed plots containing data points for each of the curves are presented in Appendix I. The plot of shield areal density vs. bumper areal density shows that none of the materials examined have the same optimum bumper areal density as 6061-T6 aluminum (the bumper material used as standard for the constant areal density investigation) but that all the optimum areal densities are quite close to that of aluminum. In the worst case, steel, a 5% reduction in shield areal density would have resulted if the optimum bumper thickness had been employed rather than the bumper thickness required to produce the arbitrarily-chosen standard areal density. Thus, no indication exists that the use of non-optimum bumper thicknesses are responsible for either the qualitative or quantitative aspects of the bumper areal density plot presented in Figure 1.

The results of plotting rear plate areal densities vs. bumper densities (Figure 8) show that two distinct types of behavior are present.

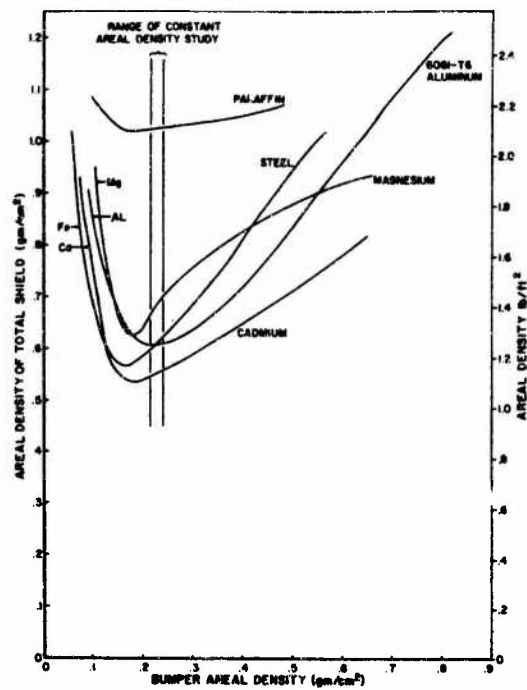


Figure 7. Total Shield Areal Density vs. Bumper Areal Density for Five Representative Bumper Materials

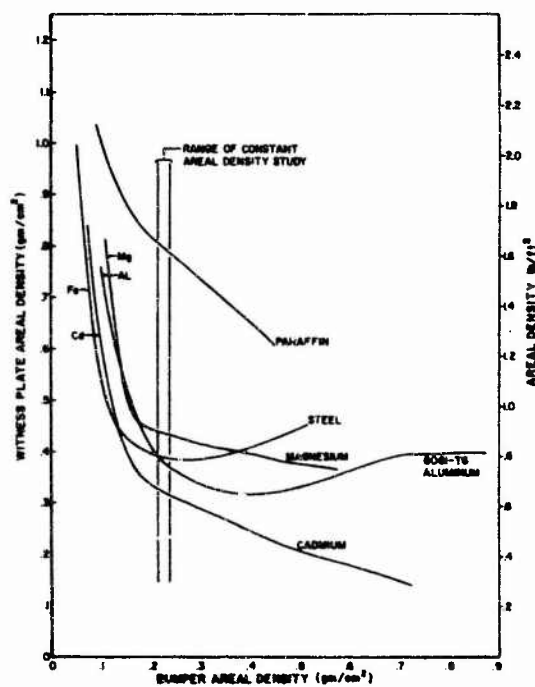


Figure 8. Witness Plate Areal Density vs. Bumper Areal Density for Five Representative Bumper Materials

Steel and 6061-T6 aluminum show definite although broad minima indicating the existence of optimum thicknesses for producing minimally destructive debris clouds. On the other hand, the destructive potential of debris clouds generated by impacted paraffin and cadmium bumpers monotonically decrease with increasing bumper areal density. The available data for magnesium bumpers does not cover a sufficient range to determine its behavior but it appears to be near a transition between the two groups.

IV. DISCUSSION

The entropy trapping arguments used to predict the physical state of debris clouds behind impacted bumpers and the arguments pertaining to debris cloud spreading can be employed to explain most of the experimental results discussed above. The following is a resume of the experimental results that must be accounted for by any successful analysis of bumper operation. Many bumper materials with material densities greater than 2 gm/cc obey the constant-area-density rule (i. e. bumpers with identical areal densities produce equally destructive debris clouds behind them when subjected to identical hypervelocity impacts). Bumper materials with notably high sublimation energies are less effective than the constant-area-density rule suggests and materials with distinctly low sublimation energies are more effective. Bumpers made from materials with densities below 2 gm/cc deviate sharply from the constant-area-density rule. In this material density region, bumper material effectiveness degenerates rapidly with decreasing material density. Optimum bumper thicknesses exist for all materials examined when the areal density of the complete shield (bumper plus rear plate) is employed as the dependent variable. The bumper materials fall into two groups, one showing optimum bumper thicknesses and one not, when cloud destructive potential (rear plate ballistic limit thickness) is chosen as the dependent parameter. Finally, no change in the destructive potential of debris clouds can be traced to the other physical properties of the bumper materials or their microstructures.

Operational Hypothesis and Related Observations

The following explanation of the experimental results has been adopted as a working hypothesis. The rate of debris cloud divergence from the original pellet trajectory and the physical state of the debris cloud material are the most crucial parameters controlling debris cloud damage potential. When both the pellet and bumper materials are liquified by impact-induced shock waves, the constant-area-density rule describes bumper performance. Similar areal density rules employing

different values of bumper efficiency may describe the behavior of bumper-pellet systems where the bumper material remains solid or vaporizes but where the pellet material is melted. Bumper materials with high sublimation energies used for this study (Ni and Ta) were not melted by the impact shock waves. The rear plates behind these bumpers exhibited small-deep craters indicating impact by relatively large, high density fragments (see Figure 4). These fragments are almost certainly bumper material. The low-sublimation-energy bumper materials (Cd and Pb) were vaporized by the impact induced shock waves while the pellet material was melted. The resulting debris clouds made up of liquified pellet material and vaporized bumper materials were correspondingly less destructive (see Figure 3). Note that both of these effects arising from bumper material states are relatively minor. The maximum deviations observed from the constant-area-density behavior were 25% in the region of the plot where bumper density exceeded 2 gm/cc. The relative insensitivity of the debris cloud destructiveness to bumper material state changes arises from the fact that the energetic bumper material makes up a relatively minor fraction of the total debris clouds. Almost all the energetic bumper material in the debris cloud comes from a cylinder within the bumper whose diameter approximates that of the pellet. Since all bumpers considered have equal mass per unit areas, the masses of all these cylinders are approximately equal and contain approximately 27% of the total debris of the cloud mass. Thus, the major portion of the debris clouds consists of pellet material which is in the same state (molten) in all cases considered.

Pellet impacts with bumper materials whose density is less than 2 gm/cc do not produce sufficiently intense shock waves to melt the pellet material. Thus, progressively larger chunks of pellet material pass through the bumper and impact the rear plate with progressively greater destructive power as bumper densities are reduced since these reductions lead to corresponding reductions in peak shock wave pressures. The resulting progressive increase in mean crater size on the rear plates protected by bumpers with progressively lower densities can be observed in Figure 5.

No direct explanation is available for the qualitative difference between the two types of bumper thickness vs. debris cloud destructive potential plots (Figure 8). The difference in cloud destructiveness must be due exclusively to bumper materials properties since all other impact parameters were held constant. The variation was observed to correlate with whether the bumper material vaporized (Cd, paraffin) or melted (Al, Fe), but could also be correlated with gross material strength, and a number of other strength-related parameters.

The only bumper material parameters that were found to affect particle shield operation were the density, fusion energy, and sublimation

energy of the materials. In particular, wide variations of material static strengths, ductility, and high strain rate behavior had no discernible effect upon shield performance. Since bumper operation is not affected by bumper material strength and high strain rate parameters, the high energy components of the debris cloud must determine its destructive potential. Material strength parameters affect the components of the debris cloud launched during the later stages of the hole growth processes but have no effect upon early-time processes where typical pressures are two to three orders of magnitude greater than materials strengths.

Shock Wave Heating Evaluation

The most revealing test of the operating hypothesis discussed above is to compare the experimental indications of pellet and bumper material states in debris clouds with predictions developed from nonrelated experiments and fundamental theory of shock waves in solids. The peak pressures generated have been approximated by those generated during the impact of two parallel half spaces, one made from pellet material and the other from bumper material. Arguments justifying this approximation are presented in Appendix II. Local areas within a spherical pellet experience pressure augmentation and reduction due to shock focusing but their overall effects are insignificant. Appendix II contains a short discussion of the theory and techniques required for computing one-dimensional shock pressure. Necessary inputs for these computations are the shock-dynamic equations of state for the participating materials and empirical Hugoniot data which for many common materials are currently available^(12, 13). These data plus the techniques presented in Appendix II were used to generate the peak pressure vs. bumper material density plot presented in Figure 9. Note that the peak shock wave pressure for aluminum pellets impacting various materials rises almost monotonically with increasing material density. A monotonically increasing band (shaded area of Figure 9) contains all the materials used in this study. Finally, note the miniscule value for the estimated dynamic shear strength of the aluminum pellets. This strength, typical of the pressure required to deform a pellet, is less than 2.5% of the lowest peak shock wave pressures considered.

Appendix II also contains a description of the technique used to evaluate the residual heating of materials exposed to shock waves. Several sources for this data are currently available but they do not agree closely with one another. This difficulty arises because little accurate data concerning the fusion and sublimation energies of materials

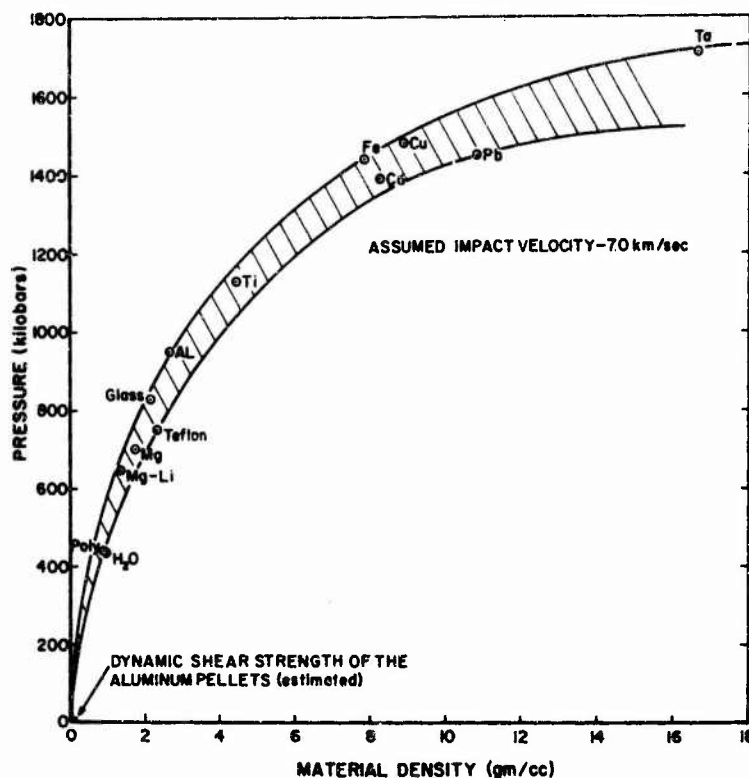


Figure 9. Peak Shock Impact Pressure Generated by Aluminum Pellet Impact vs. Bumper Material Density. Shock Pressures Were Computed From One-Dimensional Impact Analysis.

is currently available. Another smaller effect contributing to the lack of agreement between investigators is the lack of accurately determined equations of state for the materials used for this study. Complete equations of state are needed to compute the pressure-density profile followed by shock compressed material as it returns to zero pressure along an isentropic path. The presently available data concerning shock heating of materials used for this study is presented in Table IV. The double values for material melting and vaporization occur because of the finite energy required to melt or vaporize material once it has been heated to the melting or boiling points. Figure 10 is a plot of temperature vs. internal energy for a crystalline material extending from the solid through the gaseous states. The relative energies required to cause incipient and complete melting, and vaporization are indicated.

Table IV also presents the impact velocities of aluminum pellets required to melt and vaporize the bumper materials. Data from this table were used to determine the conditions of pellet and bumper material in debris clouds presented in Table I. Figure 11 is a replot of rear plate ballistic limit thickness vs. bumper density for the constant bumper areal density study where the pellet and bumper material states in the debris clouds are indicated. Note the agreement between the

TABLE IV

Shock Heating Data for Some Materials Used for the Bumper Materials Effects Study

Material	Melting				Vaporization				Source
	Incipient		Complete		Incipient		Complete		
	Pressure Mb	Al Impact Velocity km/sec	Pressure Mb	Al Impact Velocity km/sec	Pressure Mb	Al Impact Velocity km/sec	Pressure Mb	Al Impact Velocity km/sec	
Magnesium	0.48	5.40							A
Aluminum	0.70	5.60	1.00	7.0					A
	0.67	5.50	0.88	6.6	1.67	10.2	4.70		B
	0.61	5.10	0.85	6.5					C
Titanium	1.30	7.60							A
Iron (Steel)	1.80	7.90	2.10	8.80					A
Cadmium	0.33	2.50	0.46	3.20					A
	0.40	3.0	0.59	3.9	0.88	5.2	1.80	8.1	B
	0.33	2.5	0.43	3.15	0.70	4.4	5.30		C
Copper	1.40	6.60	1.84	8.00					A
	1.40	6.60	1.84	8.00	3.40	12.6	34.00		C
Nickel	2.3	9.00							A
Lead	0.25	2.00	0.35	2.60					A
	0.27	2.1	0.34	2.5	0.84	4.8	2.30	9.1	B

A - Ref. 10.

B - R. Kruger, Systems, Science and Software Company, San Diego, California, personal communication.

C - M. Rosenblatt, Shock Hydrodynamics, Incorporated, Sherman Oaks, California, personal communication.

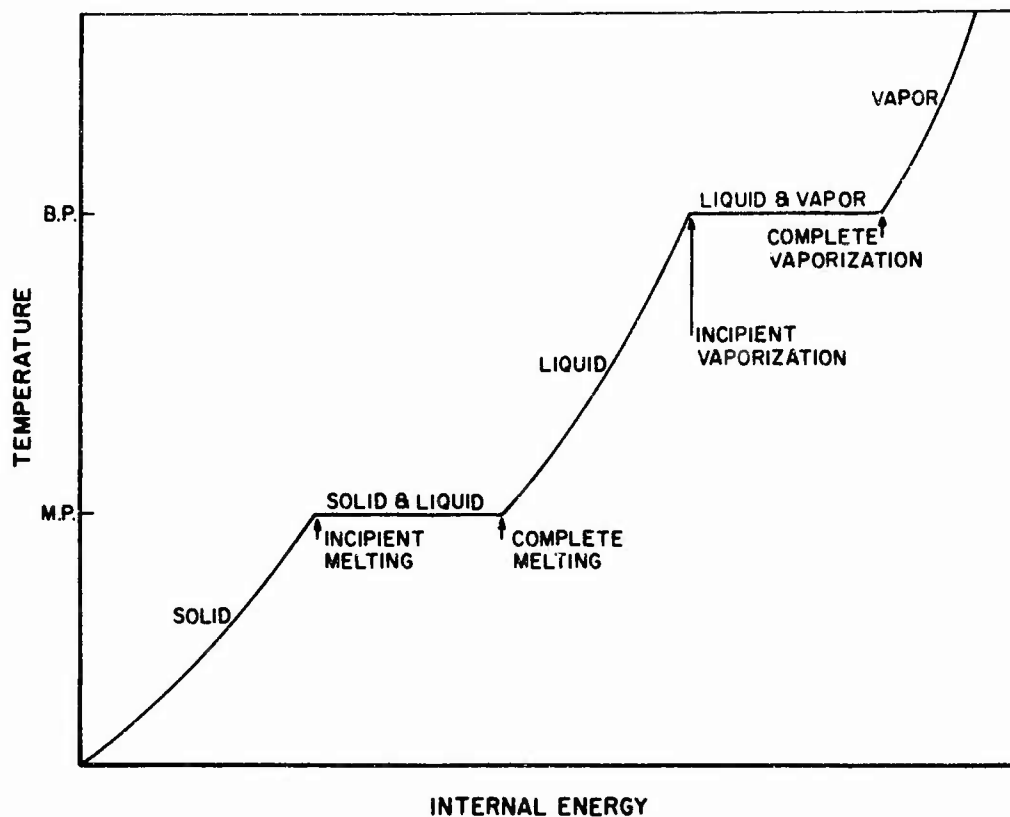


Figure 10. Temperature vs. Internal Energy of an Arbitrary Crystalline Material Showing Melting and Vaporization

operational hypothesis and the experimental results, i. e. (1) materials where pellets and bumper melt following a constant-area-density rule; (2) bumper materials that vaporize or fail to melt fall below or above the constant-area-density line, respectively; (3) bumper effectiveness drops rapidly with reducing bumper density once peak shock pressures fall below those required to melt the aluminum pellets.

V. CONCLUSIONS

The conclusions of this report must be considered in the light of current information pertaining to the operation of bumpered particle shields. First, the shock heating analysis described above appears to be a valid description of the phenomena controlling bumper particle shield response to hypervelocity impact. The constant-area-density rule for predicting bumper performance has been validated at least for the cases where both pellet and bumper materials making up the debris clouds are liquid. That absolute shifts occur in bumper effectiveness between bumpers whose debris cloud material remains solid, melt, or vaporize has been substantiated. Indications are strong that other constant-area-density rules with different values of overall

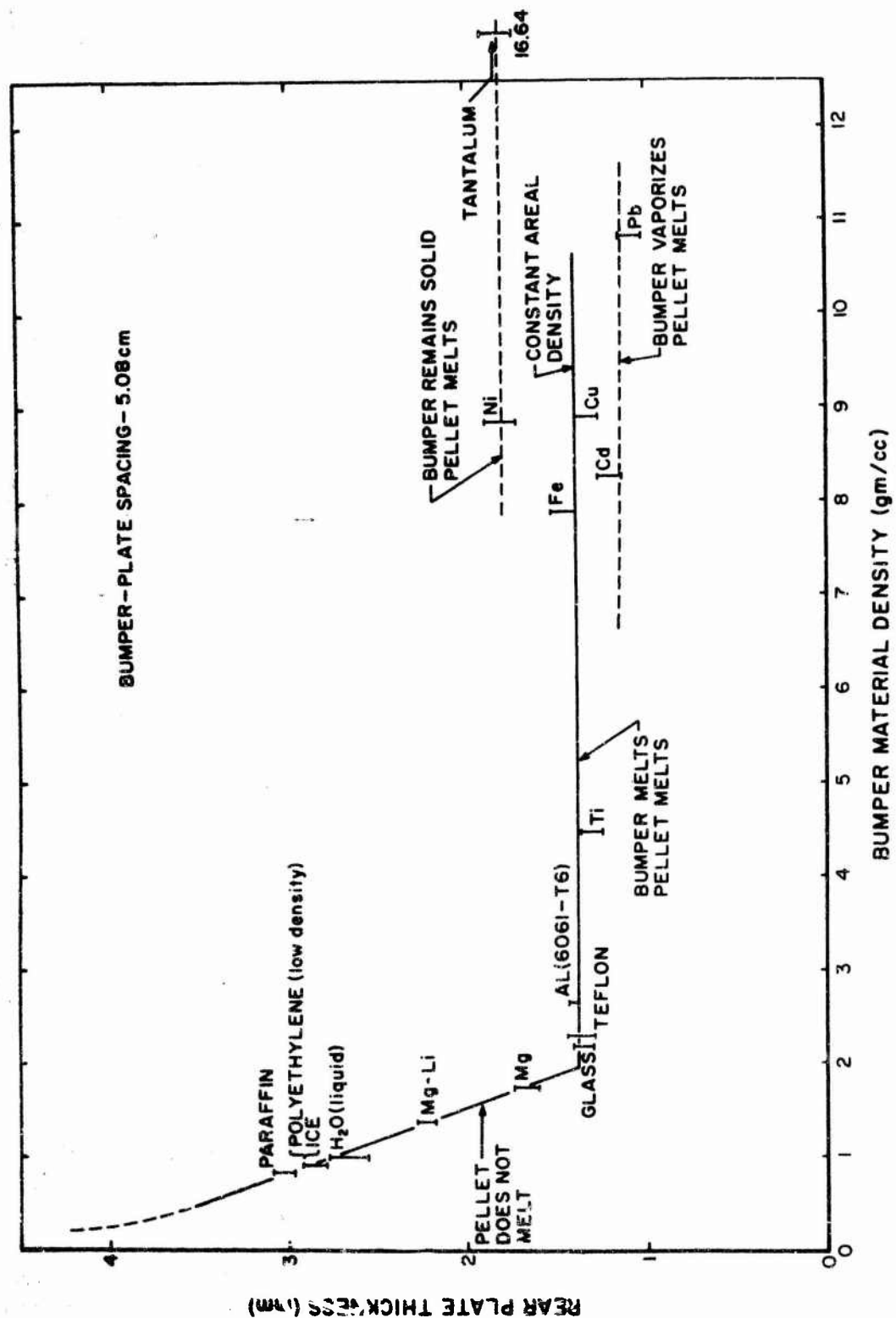


Figure 11. Data Plot for Constant Bumper Areal Density Study Showing States of Bumper and Pellet Materials in the Debris Clouds

effectiveness can be established to describe shield operation for cases where the shocked bumper material remains solid or is vaporized.

Changes in the state of pellet material in debris clouds have been shown to exert the strongest influence on bumpered shield performance of any parameters investigated. Bumper effectiveness drops rapidly with decreasing peak shock wave pressure once these pressures were reduced to values below those required to melt the incoming pellet. Peak shock wave pressures were controlled by varying bumper densities. It would be of interest to adjust these pressures in the future by changing impact velocities. The arguments concerning pellet material state would be strengthened further if the velocity dependence of shifts in the minimum bumper density required to achieve compliance with constant-area-density rules could be predicted.

Finally, the question of bumpered particle shield behavior when incoming pellets are vaporized by bumper impacts is of extreme importance. The question of whether another sharp increase in bumper effectiveness occurs when the pellet is vaporized by the impact is still open. Experimental studies of this regime can be accomplished by employing pellets made from low-sublimation-energy materials such as cadmium, tin, zinc, or plastics that can be vaporized by currently-attainable shock pressures. Any significant excursion of these results from those obtained when impacting pellets are melted would be of extreme practical as well as fundamental significance.

Many lower velocity meteoroids and man-made pellets will be melted by encounters with space vehicle bumpers whereas the higher velocity pellets will be vaporized. Practical bumpered particle shields must be capable of withstanding impacts from pellets that will be either melted or vaporized by the impact-induced shock wave.

Future studies will pursue the effects of bumper spacing and foam or other energy absorbing fillers on the ballistic limits, especially with regard to their modification to the physical state of the debris clouds.

REFERENCES

1. Whipple, F. L., "Meteoric Phenomena and Meteorites", in Physics and Medicine of the Upper Atmosphere, edited by C. S. White and O. O. Benson, Jr., University of New Mexico, Press, Albuquerque, New Mexico, 1952.
2. Swift, H. F., Carson, Lt. J. M., and Hopkins, A. K., "Ballistic Limits of 6061-T6 Aluminum Bumper Systems", Technical Report AFML-TR-67-324, October 1967.
3. McMillan, A. R., "Experimental Investigations of Simulated Meteoroid Damage to Various Spacecraft Structures", General Motors Corporation, NASA-CR-915, January 1968.
4. Zwarts, F. A., "The Initial One-Dimensional Expansion of the Shocked States Generated by the Impact of Cylindrical Pellets With Thin Plates", McGill University, NASA-CR-54209, January 15, 1965.
5. Rolsten, R. F., Hunt, H. H., and Wellnitz, J. N., "Study of Principles of Meteoroid Protection", General Dynamics/Astronautics Corp., Report AE62-0413, April 1962.
6. Maiden, C. I., "Experimental and Theoretical Results Concerning the Protective Ability of a Thin Shield Against Hypervelocity Projectiles", Sixth Symposium on Hypervelocity Impact, August 1963.
7. Riney, T. D. and Halda, E. J., "Effectiveness of Meteoroid Bumpers Composed of Two Layers of Distinct Materials", Journal of the AIAA, Vol. 6, No. 2, pp. 338-343, February 1968.
8. Rolsten, R. F., Wellnitz, J. N., and Hunt, H. H., "An Example of Hole Diameter in Thin Plates Due to Hypervelocity Impact", Journal of Applied Physics, Vol. 35, No. 3, pp. 556-559 (1964).
9. Carson, Lt. J. M. and Swift, H. F., "Hole Diameters in Thin Plates Perforated by Hypervelocity Projectiles", Technical Memorandum AFML/MAY-TM-67-9, November 1967.
10. Bjork, R. L. and Olshaker, A. E., "The Role of Melting and Vaporization in Hypervelocity Impact", RAND Corporation, Memorandum RM-3490-PR, May 1965.

11. Carey, D. A., "An Investigation of the Debris Cloud Produced by the Impact of Spheres on Thin Metal Sheets", Master's Thesis, Air Force Institute of Technology, WPAFB, GSF/Mech 67-1, June 1967.
12. Rice, M. H., McQueen, R. G., and Walsh, J. M., "Compression of Solids by Strong Shockwaves", Los Alamos Scientific Laboratory, Los Alamos, New Mexico.
13. Van Thiel, M., "Compendium of Shockwave Data, Sections B, C, D, Index", Lawrence Radiation Laboratory, University of California, Livermore, California, Report No. UCRL-50108 (Vol. 2), June 1966.
14. Swift, H. F., "The Air Force Materials Laboratory Hypervelocity Ballistic Range", AFML Technical Report No. AFML-TR-67-2, January 1967.
15. Walker, F. E., "A Fortran Program (TEMCAL) for Calculation of Hugoniot Temperature Isotherms, and Release Adiabats From Hydrodynamic Data", Lawrence Radiation Laboratory, University of California, Livermore, California, Report No. UCRL-50210, March 1967.

APPENDIX I

SUPPORTING DATA

This appendix consists of a computer printout listing pertinent parameters of all AFML gas gun firings whose data were used in this investigation (Table V) plus detailed plots of several curves presented in the main text showing individual data points (Figures 12-16). A large fraction of the firings were carried out for other purposes but were found to be applicable for this investigation. All the data is tabulated in hybrid MKS-CGS units but English engineering units are included on some graphical plots as appropriate. The densities of all materials used in this investigation were measured directly. Note that the reported densities deviate from handbook values in several instances. Pellet velocities were measured using a perpendicular-slit streak camera system described in a previous report⁽¹⁴⁾. All other measurement techniques are straightforward.

TABLE V

Firing Data for All Gas Gun Rounds Used for the Bumper Materials Effects Study

MATERIAL	BUMPER		HULL		TOTAL MASS/AREA (GM/CM ²)	PROJECTILE		RESULTS	
	DENSITY (GM/CC)	THICKNESS (CM)	MASS/AREA (GM/CM ²)	THICKNESS (CM)		MASS (MG)	VELOCITY (KM/SEC)	SPRAY CONE D. (CM)	HULL PERF. NO.
PARAFFIN	0.94	0.160	0.134	0.317	0.982	45.90	7.25	6.07	2327
		0.150	0.134	0.369	1.118	45.77	7.25	7.45	2326
		*0.254	0.213	0.282	0.966	46.04	6.29	5.70	2310
		*0.254	0.213	0.295	1.000	45.72	6.10	5.27	2320
		*0.254	0.213	0.307	1.034	45.88	6.38	5.13	2319
		*0.254	0.213	0.317	1.061	46.12	6.42	5.59	2311
		0.317	0.257	0.279	1.013	45.88	7.30	5.59	2328
		0.475	0.390	0.203	0.942	45.73	6.25	5.38	2332
		0.475	0.390	0.229	1.009	45.72	7.14	4.97	2334
		0.474	0.400	0.257	1.085	45.58	7.18	4.83	2329
ICF	0.92	0.226	0.208	0.290	0.982	46.18	6.22	5.42	2315
		0.226	0.208	0.317	1.056	45.70	6.32	5.32	2316
		0.226	0.208	0.320	1.063	45.86	7.34	5.80	2322
		0.226	0.208	0.330	1.090	45.78	7.27	5.02	2325
		0.226	0.208	0.343	1.124	45.92	7.26	5.94	2324
		0.226	0.208	0.354	1.163	45.76	7.26	6.03	2323
		*0.246	0.227	0.279	0.973	45.76	7.04	5.16	2359
		*0.246	0.227	0.292	1.007	45.72	7.25	5.97	2360
		*0.236	0.219	0.145	0.605	47.40	7.07	6.40	2273
		*0.236	0.219	0.254	0.897	48.00	7.04	5.05	2278
POLYETHYLENE	0.92	*0.236	0.219	0.263	0.937	45.76	6.37	5.30	2292
		*0.236	0.219	0.282	0.971	45.90	6.20	5.13	2308
		*0.236	0.219	0.292	0.998	45.82	6.81	5.98	2304
		*0.234	0.234	0.257	0.919	45.92	6.54	5.05	2299
WATER	1.00	*0.234	0.234	0.279	0.980	45.77	6.70	5.27	2301
		*0.234	0.234	0.279	0.980	45.77	6.70	5.27	2301
MG-LI ALLOY	1.37	0.157	0.216	0.193	0.731	45.80	6.61	7.82	2306
		0.157	0.216	0.203	0.758	45.66	6.80	7.04	2298

* Firing used for the constant-area-density study.

Table V (Continued)

MATERIAL	BUMPER		HULL		TOTAL MASS/AREA (GM/CM ²)	PROJECTILE			RESULTS	
	DENSITY (GM/CC)	THICKNESS (CM)	THICKNESS (CM)	MASS/AREA (GM/CM ²)		MASS (MG)	VELOCITY (KM/SEC)	ENERGY (JOULES)	SPRAY CORE D. PERP. (CM)	RUNNO NO.
MAGNESIUM	1.76	0.197	0.203	0.343	0.758	46.00	6.37	932.	7.32	2294
		0.157	0.218	0.383	0.799	45.96	6.56	988.	8.22	2300
		0.157	0.216	0.610	0.826	45.78	6.84	1071.	6.67	2297
		0.157	0.241	0.644	0.860	45.82	6.51	971.	6.57	2296
		0.160	0.219	0.387	0.606	47.80	7.02	1177.	5.69	2275
		0.160	0.219	0.678	0.897	47.80	6.81	1108.	5.90	2276
		0.069	0.121	0.468	0.589	45.70	6.59	992.	6.09	2451
		0.069	0.121	0.644	0.765	45.58	6.89	1083.	6.64	2452
		0.069	0.121	0.719	0.840	45.84	6.90	1091.	6.48	2453
		0.104	0.181	0.427	0.611	45.74	7.14	1167.	6.67	2416
GLASS	2.19	0.127	0.160	0.427	0.651	45.92	7.08	1151.	6.26	2369
		0.127	0.203	0.543	0.766	45.78	6.96	1108.	6.62	2368
		0.127	0.241	0.644	0.868	45.86	7.36	1242.	6.89	2366
		0.317	0.127	0.339	0.898	45.80	7.01	1125.	6.50	2444
		0.317	0.190	0.509	1.067	45.79	6.88	1084.	7.62	2443
		0.077	0.157	0.420	0.590	45.75	6.97	1110.	8.99	2164
TEFLON	2.31	0.104	0.130	0.346	0.574	48.40	6.54	1037.	6.76	2291
		0.104	0.142	0.380	0.608	47.40	6.78	1088.	7.58	2279
		0.104	0.142	0.380	0.608	48.20	6.79	1110.	8.46	2285
		0.051	0.178	0.475	0.592	45.92	6.88	1086.	6.69	2447
		0.051	0.229	0.610	0.728	45.80	6.85	1074.	6.60	2448
		0.051	0.267	0.712	0.829	45.78	6.83	1069.	6.38	2449
		0.099	0.132	0.353	0.581	48.40	6.82	1125.	7.86	2274
		0.099	0.145	0.387	0.615	48.00	7.11	1213.	8.18	2272
		0.236	0.063	0.170	0.715	45.84	6.94	1105.	9.21	2454
		0.236	0.063	0.170	0.715	45.85	6.89	1090.	10.43	2490
		0.236	0.084	0.224	0.769	45.72	6.92	1094.	9.19	2491
		0.236	0.094	0.224	0.769	45.64	6.80	1054.	6.17	2446
		0.236	0.127	0.339	0.885	45.70	6.97	1109.	6.32	2445
		0.236	0.127	0.339	0.885	45.70	6.97	1109.	6.32	2445

* Firings used for the constant-area-density study.

Table V (Continued)

BUMPER				HULL		TOTAL	PROJECTILE		RESULTS		
MATERIAL	DENSITY (GM/CC)	THICKNESS (CM)	MASS/AREA (GM/CM**2)	THICKNESS (CM)	MASS/AREA (GM/CM**2)	MASS/AREA (GM/CM**2)	MASS (MG)	VELOCITY (KM/SEC)	ENERGY (JOULES)	SPRAY CONE D. (CM)	HULL PERFOR. NO.
ALUMINUM	2.67	0.041	0.109	0.145	0.387	0.495	45.80	7.32	1226.	3.44	YES
		0.041	0.109	0.157	0.420	0.529	45.76	6.16	867.	5.46	YES
		0.041	0.109	0.257	0.685	0.793	45.74	6.85	1074.	8.51	YES
		0.063	0.170	0.140	0.373	0.543	45.68	7.11	1155.	6.22	YES
		0.063	0.170	0.160	0.427	0.597	45.90	7.27	1212.	7.59	YES
		0.063	0.170	0.180	0.482	0.651	45.76	7.22	1193.	6.72	NO
		0.079	0.210	0.127	0.339	0.549	45.84	6.69	1026.	0.	YES
		0.079	0.210	0.140	0.373	0.583	45.81	6.79	1055.	5.84	YES
		0.079	0.210	0.160	0.373	0.583	45.78	6.46	956.	7.66	NO
		0.079	0.210	0.152	0.407	0.617	45.94	7.00	1127.	8.61	NO
	0.079	0.210	0.160	0.427	0.637	45.88	7.32	1228.	8.08	NO	
	0.081	0.217	0.159	0.424	0.641	45.66	7.23	1192.	10.97	NO	
	0.083	0.220	0.150	0.400	0.621	47.46	6.59	1030.	10.03	NO	
	4.46	0.084	0.224	0.084	0.224	0.448	45.78	7.26	1208.	6.50	YES
		0.084	0.224	0.084	0.224	0.448	47.54	7.13	1207.	10.73	YES
		0.084	0.224	0.104	0.278	0.502	45.82	7.11	1158.	7.11	YES
		0.084	0.224	0.127	0.339	0.563	45.79	6.93	1058.	7.34	YES
		0.084	0.224	0.140	0.373	0.597	47.52	6.42	978.	9.40	YES
		0.084	0.224	0.140	0.373	0.597	45.73	7.26	1204.	6.63	YES
		0.084	0.224	0.140	0.373	0.597	47.46	6.39	970.	9.21	YES
0.084		0.224	0.145	0.387	0.610	45.89	7.20	1191.	10.79	NO	
0.084		0.224	0.152	0.407	0.631	45.80	6.63	1007.	8.69	NO	
0.084		0.224	0.160	0.427	0.651	47.56	7.31	1271.	10.67	NO	
TITANIUM	4.46	0.104	0.278	0.127	0.339	0.617	46.00	7.23	1203.	8.55	GL
		0.104	0.278	0.140	0.373	0.651	45.74	7.27	1208.	11.38	NO
		0.160	0.427	0.079	0.210	0.637	45.78	7.25	1202.	9.02	YES
		0.160	0.427	0.127	0.339	0.766	45.74	7.27	1208.	10.54	NO
		0.160	0.427	0.160	0.427	0.855	45.78	4.55	473.	5.94	NO
		0.257	0.695	0.140	0.373	1.058	45.64	6.68	1018.	7.39	YES
		0.257	0.695	0.157	0.420	1.105	45.72	6.38	931.	12.70	NO
		0.051	0.227	0.051	0.136	0.362	45.84	7.01	1126.	7.16	YES

* Firings used for the constant-area-density study.

Table V (Continued)

NUMBER			MILL		TOTAL	PROJECTILE			RESULTS	
MATERIAL	DENSITY (GM/CC)	THICKNESS (CM)	MASS/AREA (GM/CM ²)	THICKNESS (CM)	MASS/AREA (GM/CM ²)	MASS (MG)	VELOCITY (KM/SEC)	ENERGY (JOULES)	SPRAY MILL CONE D. PERP. (CM)	TESTING NO.
STEEL	7.85	0.051	0.227	0.127	0.339	0.566	45.89	6.86	1080.	2438
		0.051	0.227	0.140	0.373	0.600	45.76	7.01	1124.	2436
		0.051	0.227	0.160	0.427	0.654	45.04	7.01	1126.	2435
	7.85	0.008	0.038	0.145	0.387	0.445	45.68	6.74	1038.	2485
		0.004	0.038	0.16	0.376	0.435	46.04	6.97	1119.	2486
		0.008	0.038	0.257	0.712	0.770	45.84	6.87	1082.	2487
	0.004	0.008	0.038	0.317	0.848	0.906	45.76	6.85	1075.	2488
		0.004	0.038	0.336	0.949	1.009	46.14	7.01	1133.	2489
		0.020	0.155	0.145	0.387	0.542	45.76	7.01	1123.	2411
	0.020	0.020	0.155	0.160	0.427	0.583	45.80	7.06	1141.	2410
		0.030	0.233	0.140	0.373	0.606	45.80	7.20	1188.	2345
		0.034	0.291	0.127	0.339	0.631	45.76	7.10	1154.	2412
CADMIUM	8.26	0.010	0.084	0.127	0.339	0.664	46.00	7.03	1135.	2414
		0.010	0.084	0.140	0.373	0.698	45.92	7.01	1127.	2413
		0.010	0.084	0.152	0.407	0.698	45.66	6.96	1105.	2442
	8.26	0.010	0.084	0.165	0.441	0.525	45.83	7.01	1126.	2430
		0.010	0.084	0.190	0.509	0.593	46.35	6.89	1100.	2431
		0.010	0.084	0.229	0.610	0.694	45.72	7.20	1184.	2432
	0.010	0.010	0.084	0.267	0.712	0.796	46.81	7.08	1224.	2433
		0.010	0.084	0.292	0.780	0.864	45.84	6.98	1117.	2434
		0.018	0.147	0.127	0.339	0.486	45.80	7.16	1175.	2419
	0.018	0.018	0.147	0.140	0.373	0.520	45.76	6.97	1112.	2421
		0.018	0.147	0.160	0.427	0.574	45.90	7.12	1163.	2420
		0.028	0.231	0.114	0.305	0.536	45.49	6.93	1093.	2415
ZINC	7.14	0.028	0.231	0.127	0.339	0.570	45.78	6.85	1074.	2493
		0.038	0.315	0.102	0.271	0.586	45.70	7.05	1136.	2418
		0.038	0.315	0.119	0.319	0.633	45.79	7.14	1162.	2417
	0.051	0.420	0.084	0.224	0.643	45.75	6.97	1112.	2423	
		0.084	0.592	0.051	0.136	0.828	46.12	6.74	1046.	2480
		0.084	0.592	0.051	0.136	0.828	46.12	6.74	1046.	2480

* Firings used for the constant-area-density study.

Table V (Continued)

MATERIAL	BUMPER		HULL		TOTAL MASS/AREA (GP/CM ²)	PROJECTILE			RESULTS		ROUND NO.
	DENSITY (GP/CC)	THICKNESS (CM)	MASS/AREA (GP/CM ²)	THICKNESS (CM)		MASS (PG)	VELOCITY (MP/SEC)	ENERGY (JCOULES)	SPRAY CONE O. (CM)	HULL PERF.	
NICKEL	8.73	0.084	0.692	0.063	0.170	45.80	7.07	1144.	6.82	NO	2440
		0.084	0.692	0.114	0.335	45.74	6.99	1116.	5.37	NO	2422
		*0.028	0.244	0.160	0.427	45.79	6.92	1097.	5.85	YES	2481
COPPER	8.78	*0.028	0.244	0.173	0.461	45.82	6.80	1058.	14.12	YES	2482
		*0.028	0.244	0.150	0.509	46.00	6.74	1045.	11.09	NO	2483
		*0.028	0.245	0.127	0.339	46.09	7.07	1150.	4.22	YES	2439
LEAD	10.82	*0.028	0.245	0.140	0.373	45.78	6.97	1112.	7.05	NO	2425
		*0.028	0.245	0.160	0.427	45.73	7.06	1138.	4.94	NO	2424
		*0.020	0.220	0.084	0.224	45.86	7.27	1211.	6.96	YES	2351
TANTALUM	16.64	*0.013	0.211	0.102	0.271	45.84	7.13	1165.	7.56	YES	2356
		*0.013	0.211	0.114	0.305	45.76	7.24	1198.	5.33	NO	2358
		*0.013	0.211	0.119	0.319	45.76	7.25	1203.	1.89	NO	2350
		*0.020	0.220	0.142	0.380	45.54	7.23	1189.	3.56	NO	2349
TANTALUM	16.64	*0.013	0.211	0.140	0.373	45.86	7.40	1256.	5.62	YES	2347
		*0.013	0.211	0.160	0.427	45.90	7.14	1171.	5.21	YES	2348
		*0.013	0.211	0.173	0.461	45.84	7.16	1176.	7.54	YES	2353
		*0.013	0.211	0.150	0.509	45.65	7.21	1188.	5.46	NO	2364

* Firings used for the constant-area-density study.

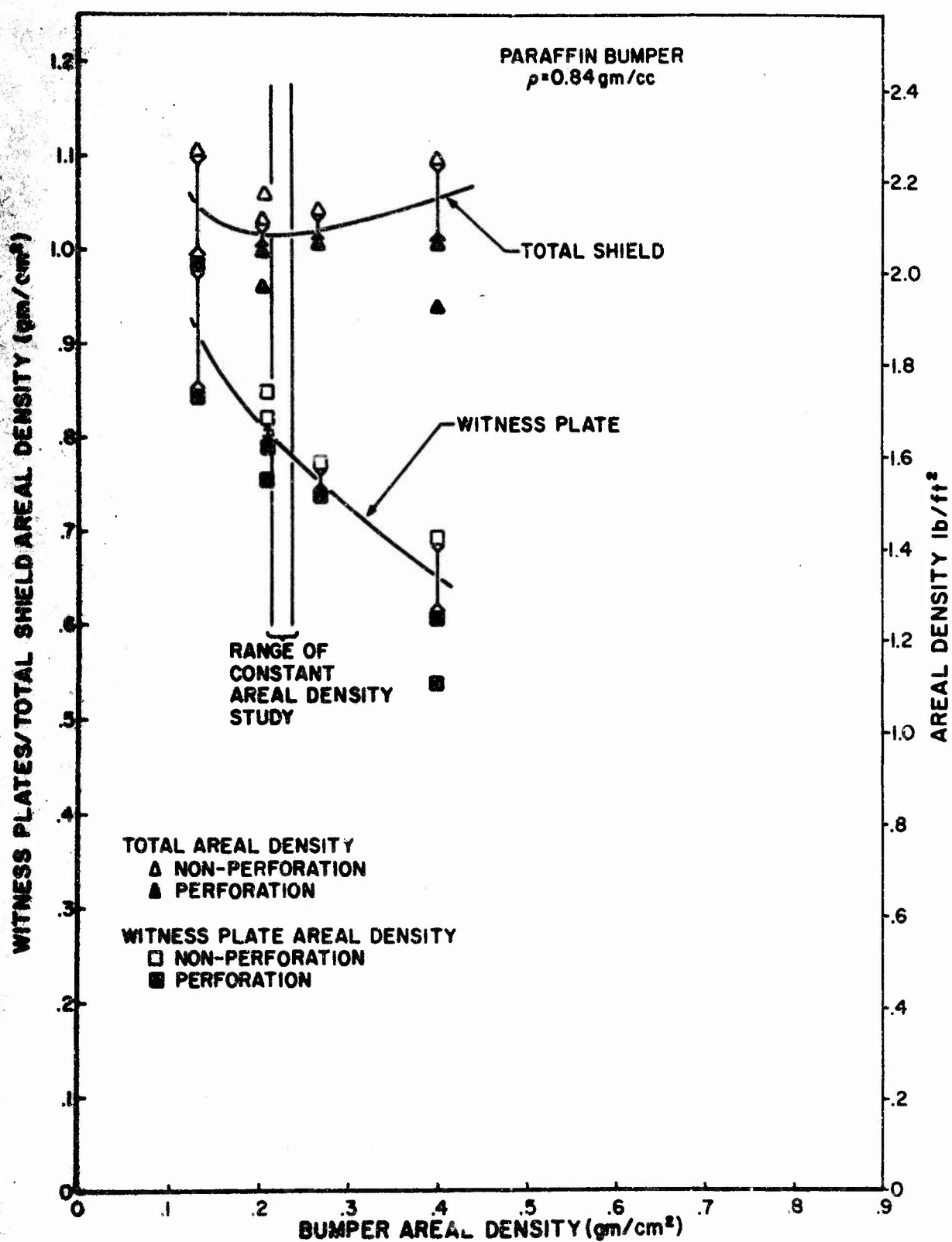


Figure 12. Areal Densities of Witness Plates and Complete Shield vs. Bumper Areal Density for Paraffin Bumpers

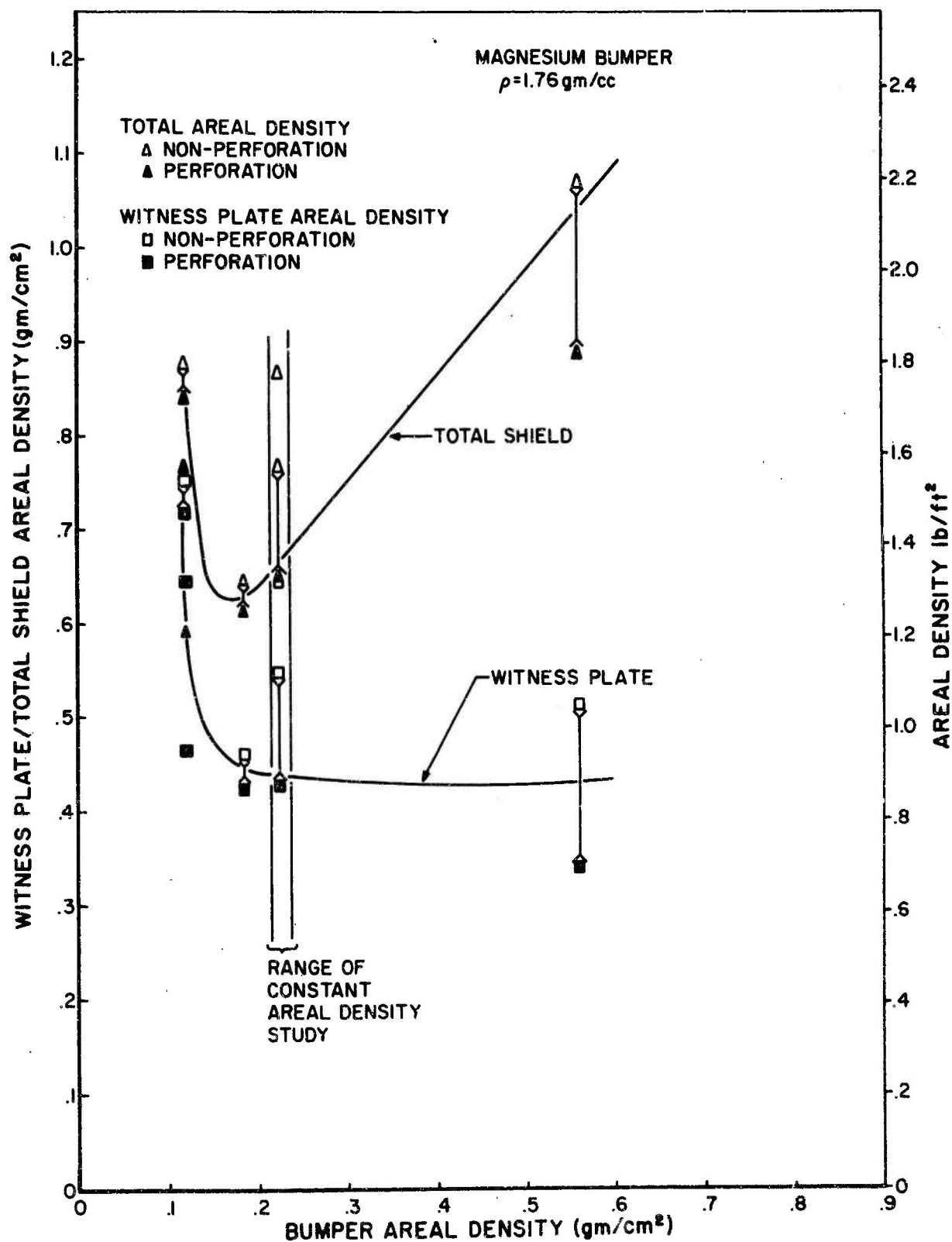


Figure 13. Areal Densities of Witness Plates and Complete Shield vs. Bumper Areal Density for Magnesium Bumpers

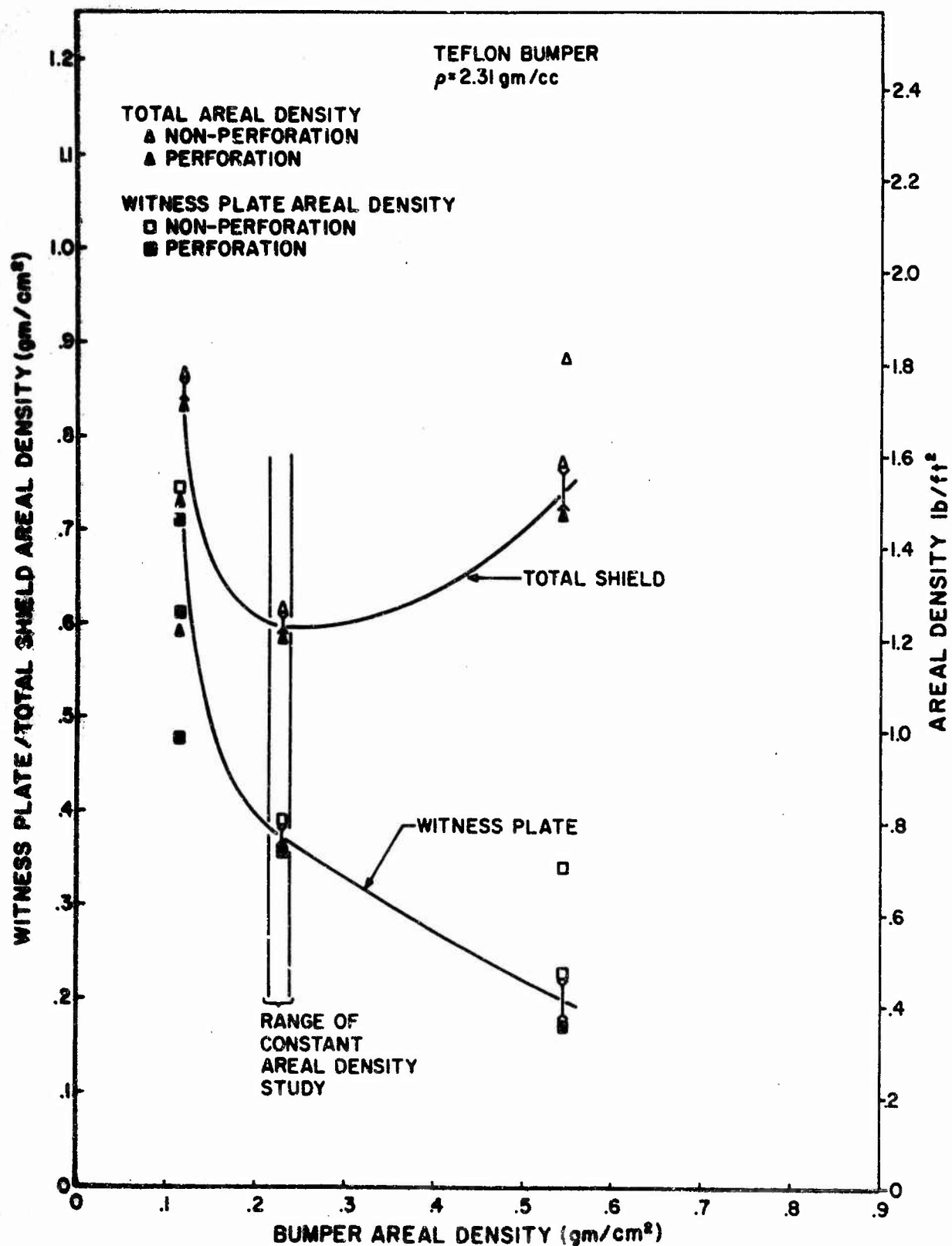


Figure 14. Areal Densities of Witness Plates and Complete Shield vs. Bumper Areal Density for Teflon Bumpers

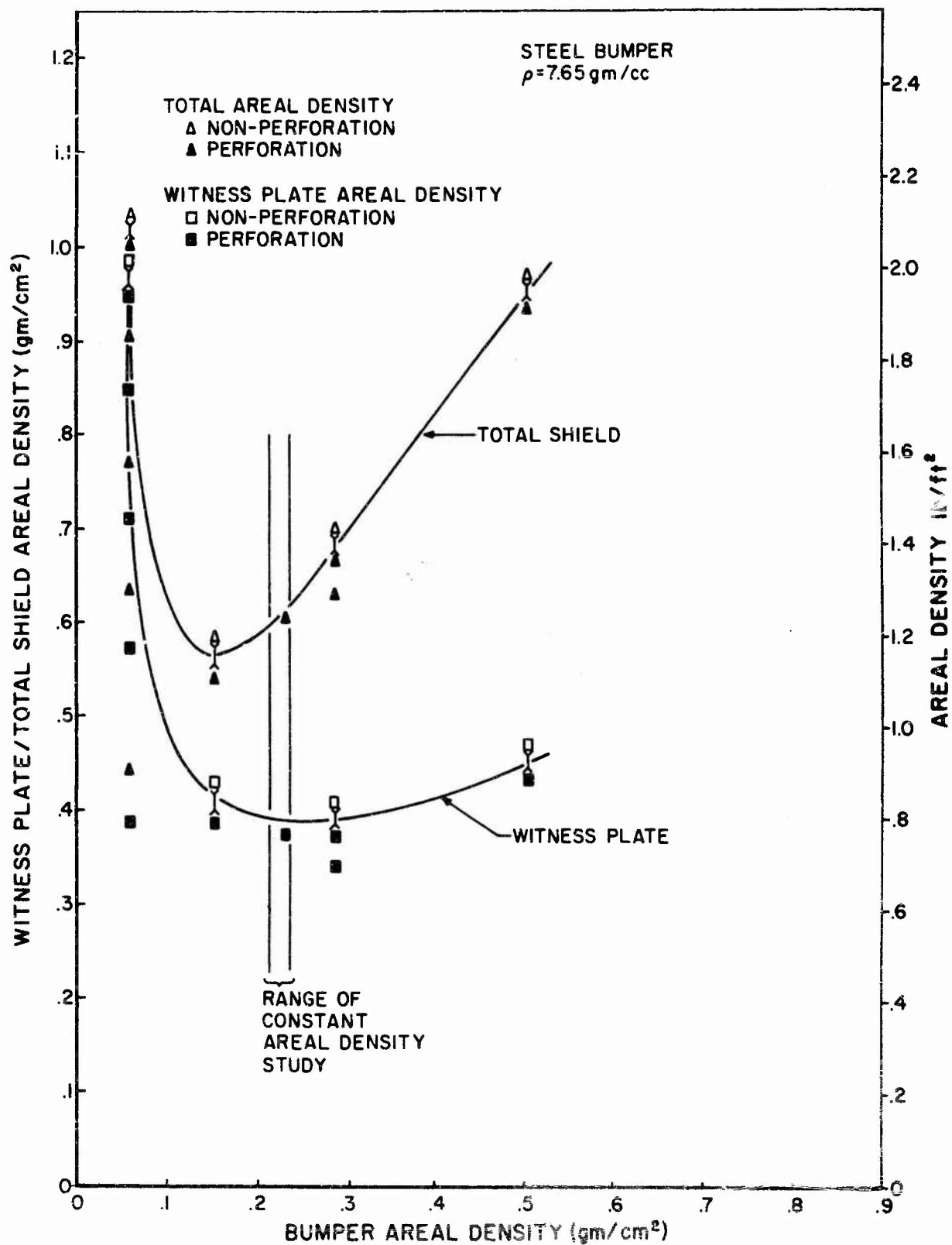


Figure 15. Areal Densities of Witness Plates and Complete Shield vs. Bumper Areal Density for Steel Bumpers

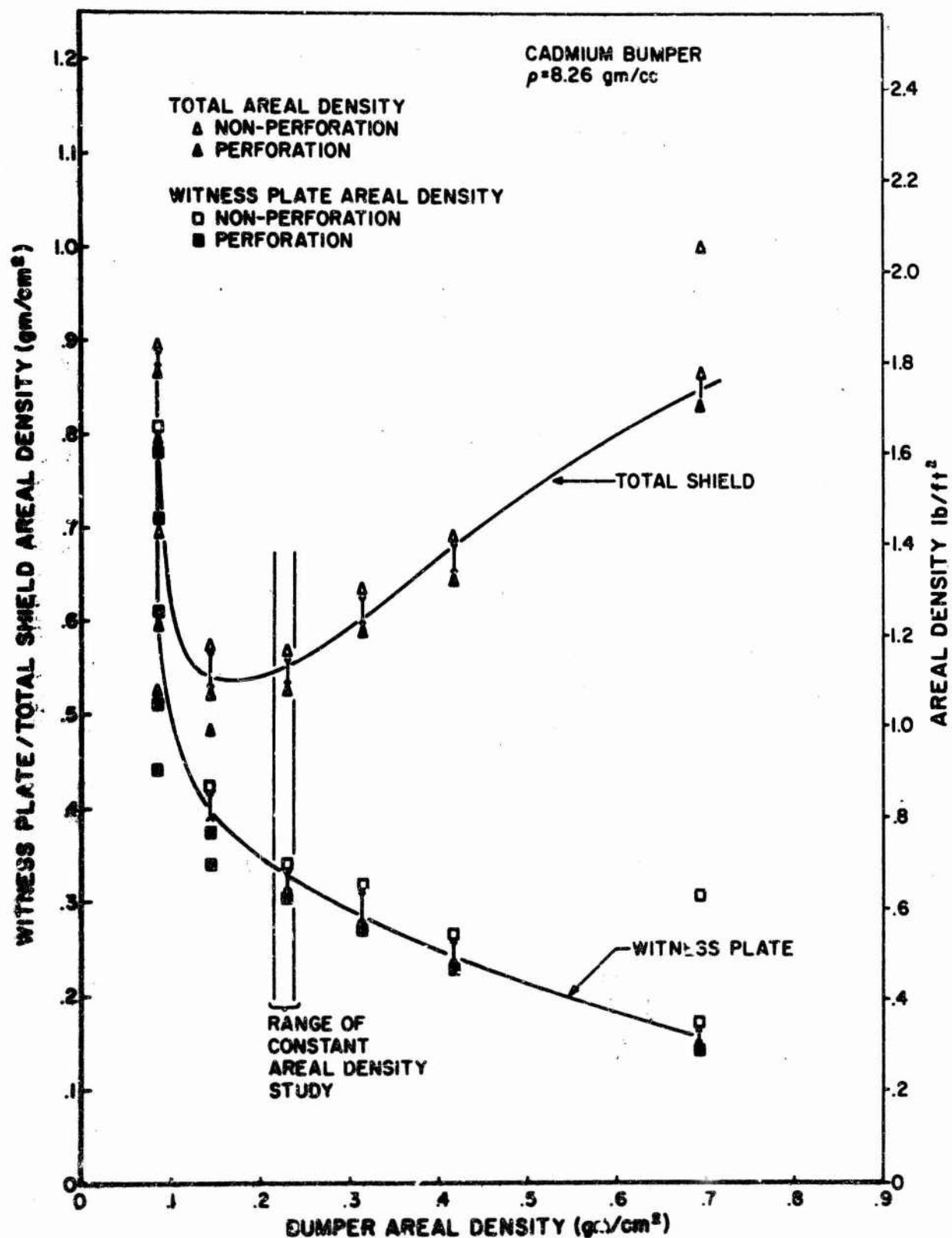


Figure 16. Areal Densities of Witness Plates and Complete Shield vs. Bumper Areal Density for Cadmium Bumpers

APPENDIX II

HYDRODYNAMIC CALCULATIONS OF PEAK IMPACT PRESSURES BETWEEN PROJECTILES AND BUMPERS

The impact of two objects at high velocities creates strong inward running shock waves in both of them. The early time characteristics of the shocks and the materials condition behind the shocks may be described by hydrodynamic relationships. Constitutive equation parameters of pressure, shock velocity, and mass velocity have been determined by planar shock experiments for a wide variety of materials. The conservation equations describing the shock and material conditions at the shock boundary are:

$$\frac{D}{V_0} = \frac{D-U}{V} \quad (\text{Conservation of Mass}) \quad (2)$$

$$P = \frac{DU}{V} \quad (\text{Conservation of Momentum}) \quad (3)$$

$$E - E_0 = 1/2 P(V_0 - V) \quad (4)$$

where

D = shock velocity

U = material velocity behind the shock

P = pressure behind the shock

V_0, V = specific volume ahead and behind the shock

E_0, E = specific internal energies in those states

The plot of the locus of states which arise when a material is compressed by shock waves of different intensity is called the shock adiabat or Hugoniot of the material. This Hugoniot may be developed from data relating any two of the parameters P, U, D, V , or V/V_0 . In Figure 17 which is the Hugoniot for aluminum, shock pressure, P , versus the material velocity, U were chosen to be plotted because this form is useful in computing pressure at a shock boundary when only the impact velocity is known. When two dissimilar materials impact, the initial

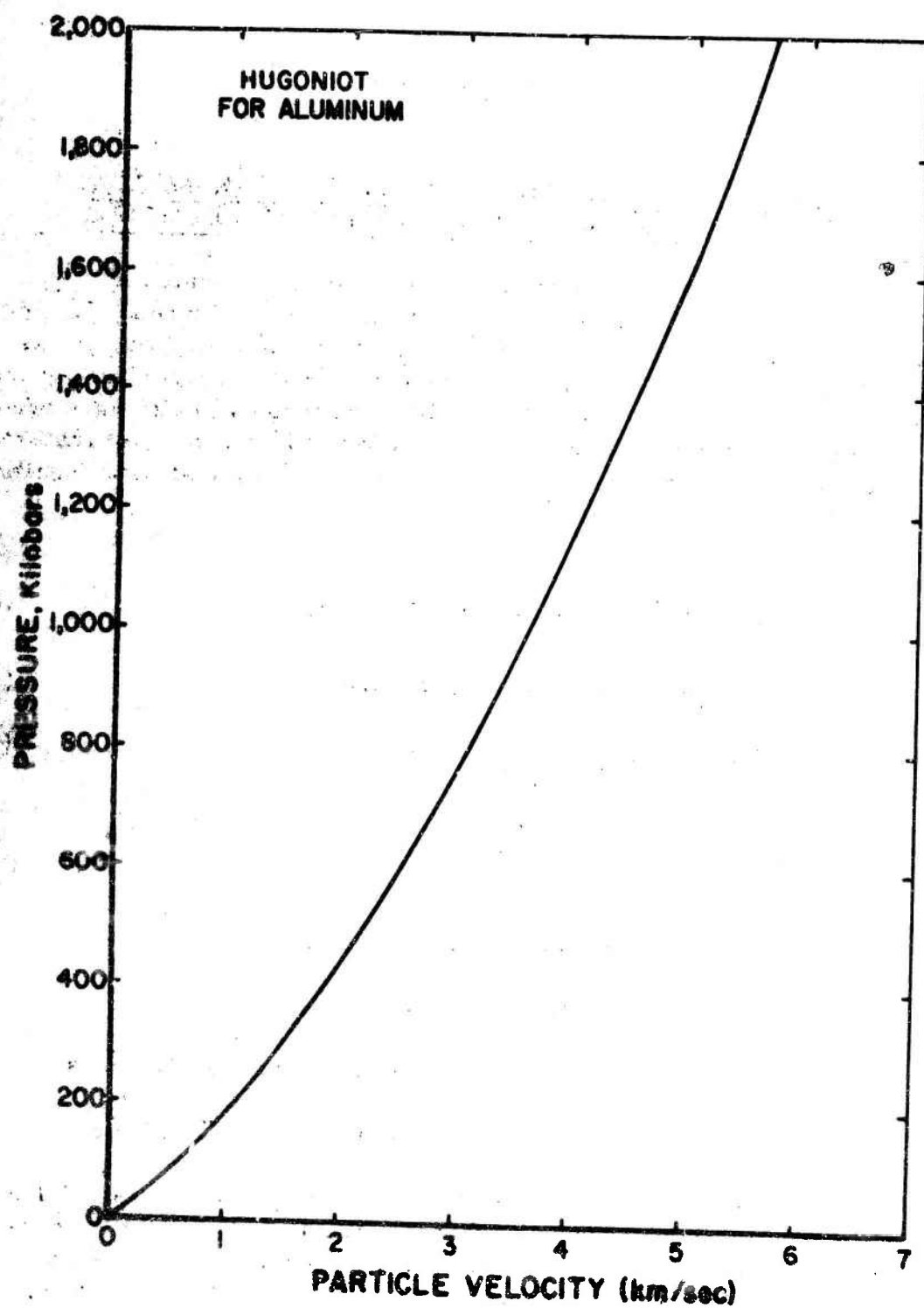


Figure 17. One-Dimensional Shock Impact Pressure of Aluminum vs. Aluminum Particle Velocity

shock wave parameters can be determined by solving the two sets of conservation equations simultaneously. This may be achieved conveniently by utilizing the reflection Hugoniot technique. Figure 18 demonstrates this process. The curves increasing upward to the right represents the compression Hugoniot for the bumper materials of interest. The curve running upward to the left is the Hugoniot for aluminum as shown in Figure 17. The abscissa of the aluminum Hugoniot has been reversed and its coordinates translated such that the impact velocity of 7 km/sec (typical of those in the experiments) is set equal to that material velocity in the pellet when the impact pressure is zero. The bumper material Hugoniot curves with the reversed aluminum curve yields the initial interface pressure between aluminum and the bumper materials and their respective mass velocities with respect to the undisturbed bumper material. This coordinate reversal and translation can be shown to yield a valid solution of the simultaneous conservation equations for the aluminum sphere and the bumper materials.

The initial interface pressures for aluminum pellets impacting each of the bumper plate materials is presented in Table VI and in Figure 9 in the main text. The rate of decay of these pressures is a function of the equation of state of the materials involved and of the geometry of the impact. The reflection technique is strictly valid only for planar impacts or for the earliest phases of spherical impacts. Edge rarefactions and shock focusing effects appear during non-planar impacts and rapidly modify the pressure profiles as time progresses. The pressures shown are the peak pressures actually achieved during these impacts. The amount of residual energy remaining in material after passage of a shock wave is dependent upon the total material equation-of-state as well as the shock Hugoniot. Equation (4) is an expression of the specific energy in shocked material. It states that this energy is equal to the area under a straight line connecting the initial and shocked material condition on a shock pressure vs. specific volume plot (Rayleigh line). The release wave which returns the material to zero pressure is very nearly isentropic. Its path from the peak pressure to zero pressure can be computed from a complete material equation-of-state by employing the constraint that the entropy of the material in the shocked state be conserved. The area under the isentrope from peak pressure to zero pressure represents the energy yielded up by the material to the ongoing shock waves. The residual energy trapped in the material is the differences between the total energy of the shocked material and that transferred out of the material by expansion or the differences between the two areas described above (see Figure 19). This energy appears as heat in previously shocked material. A computational technique for carrying out residual heat computations using a Fortran IV language computer program is described in Reference 15.

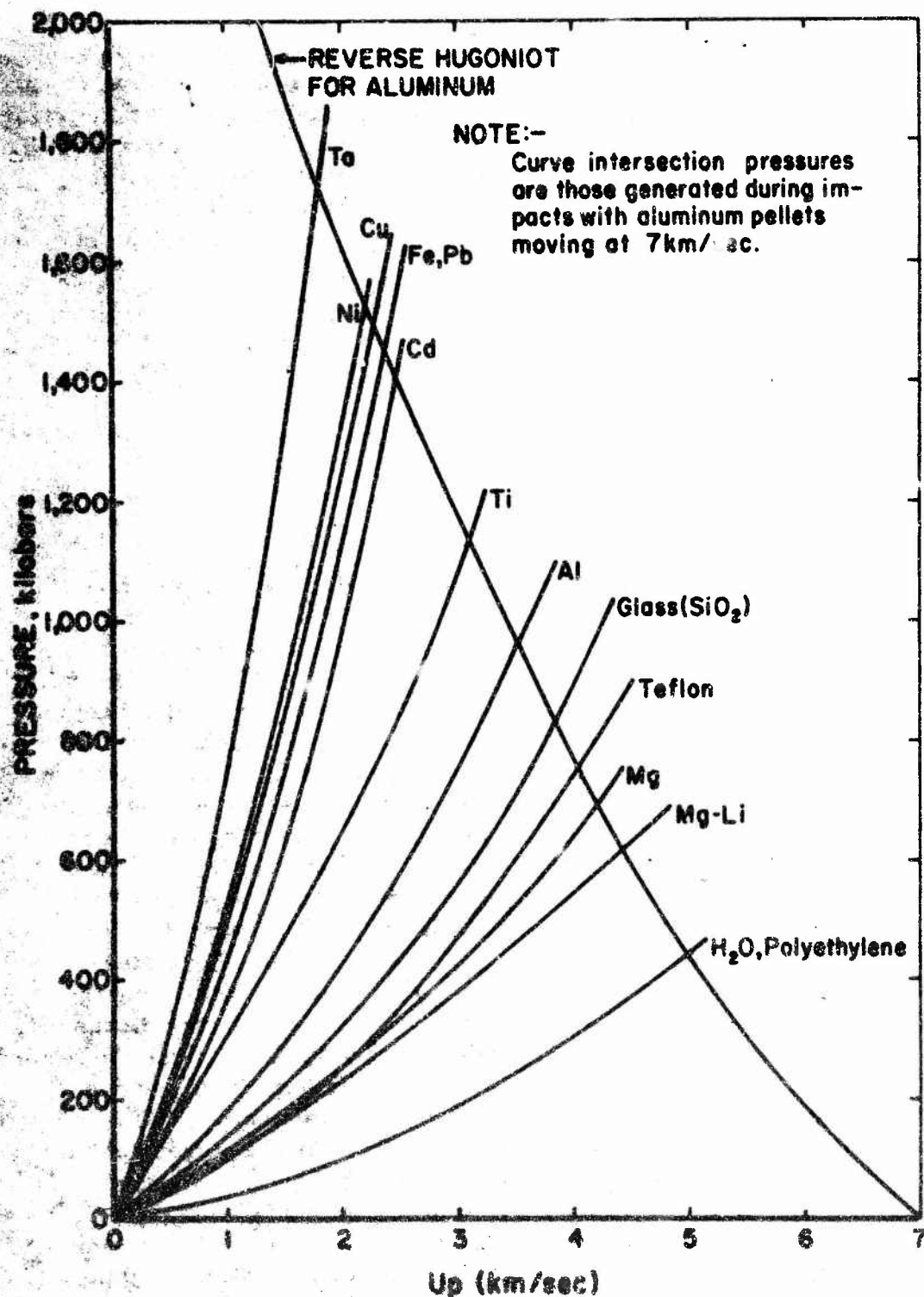


Figure 18. Shock Pressure-Particle Velocity Plots for the Bumper Materials Used in This Study. The Reverse Hugoniot Technique for Determining Impact Pressure During Impacts With Aluminum Pellets is Demonstrated.

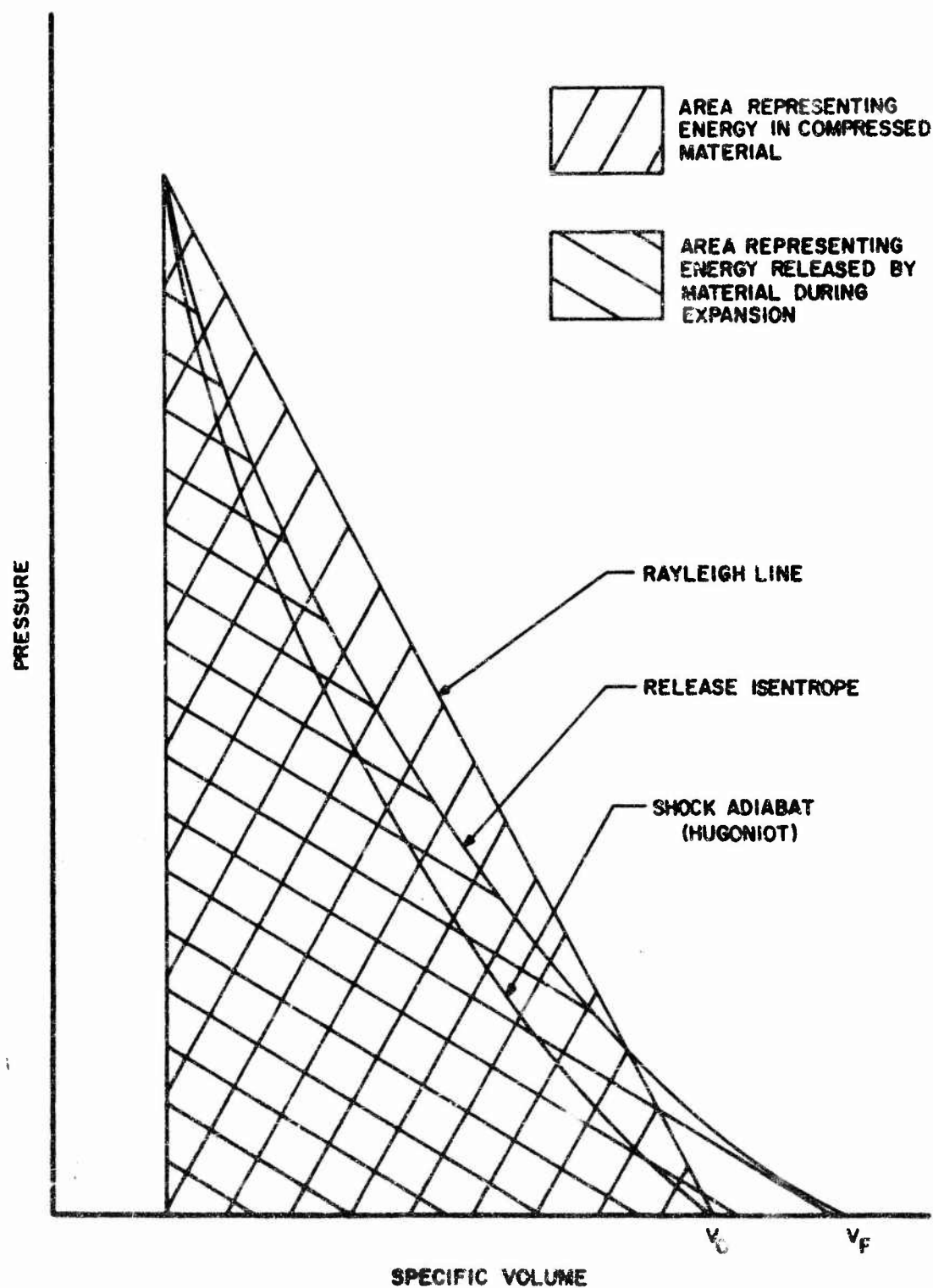


Figure 19. Shock Pressure-Specific Volume Plot for an Arbitrary Material Showing Hugoniot, Release Adiabatic, Rayleigh Line, Energy Inserted During Shock Compression and Energy Released by Material Expansion

TABLE VI

Shock Pressures Induced in Bumper Materials
When Impacted by Aluminum Pellets Traveling at 7.0 km/sec
(Pressures Calculated Using One-Dimensional Approximation)

Material	Density gm/cc	I. D. Impact Pressure Mb
Paraffin	.84	-
Polyethylene	.92	.44
Water	1.00	.44
Mg-Li (alloy)	1.37	.62
Magnesium	1.76	.70
Teflon	2.31	.76
Glass	2.19	.84
Aluminum (6061)	2.67	.965
Titanium	4.46	1.14
Cadmium	8.26	1.41
Steel	7.65	1.46
Lead	10.82	1.46
Copper	8.78	1.49
Nickel	8.73	1.53
Tantalum	16.64	1.73

~~Unclassified~~
Security Classification

DOCUMENT CONTROL DATA - R&D		
(Security classification of title, body of abstract and indexing annotation must be entered when the overall report is classified)		
1. ORIGINATING ACTIVITY (Corporate author)		2a. REPORT SECURITY CLASSIFICATION
Air Force Materials Laboratory Wright-Patterson AFB, Ohio 45433		Unclassified
		2b. GROUP
3. REPORT TITLE		
THE EFFECTS OF BUMPER MATERIAL PROPERTIES ON THE OPERATION OF SPACED HYPERVELOCITY PARTICLE SHIELDS		
4. DESCRIPTIVE NOTES (Type of report and inclusive dates)		
Technical Report on work completed during July 1968		
5. AUTHOR(S) (Last name, first name, initial)		
Swift, Hallock F. and Hopkins, Alan K.		
6. REPORT DATE	7a. TOTAL NO. OF PAGES	7b. NO. OF REFS
September 1968	42	15
8a. CONTRACT OR GRANT NO.	8a. ORIGINATOR'S REPORT NUMBER(S)	
F33615-68-C-1138	UDRI-TR-68-30	
a. PROJECT NO.	8b. OTHER REPORT NO(S) (Any other numbers that may be assigned this report)	
7360	AFML-TR-68-257	
c.		
d. Task No. 736006		
10. AVAILABILITY/LIMITATION NOTICES		
This document has been approved for public release and sale; its distribution is unlimited.		
11. SUPPLEMENTARY NOTES	12. SPONSORING MILITARY ACTIVITY	
	Air Force Materials Laboratory Air Force Systems Command Wright-Patterson AFB, Ohio 45433	
13. ABSTRACT		
<p>—> An experimental study has been conducted to evaluate the importance of bumper materials selection upon the performance of two-component hypervelocity impact bumper shields. Several bumper materials were found that were equally effective on a mass per unit area basis. Bumper material effectiveness dropped rapidly with bumper material density when this density was below 2 gm/cc. Optimum bumper thicknesses exist for minimizing total shield weight for all bumper materials investigated. All of the data obtained in this study can be explained by an analysis of the states of the impacting pellet and bumper material within the debris cloud projected behind impacted bumpers. The most important parameter controlling shield operation is the state of the pellet material in the debris cloud. () ←</p>		

DD FORM 1473
1 JAN 64

Unclassified
Security Classification

Unclassified
Security Classification

KEY WORDS

Hypervelocity Impact
Whipple Bumpers
Material Properties
Impact Shock Waves
Shock Wave Thermodynamics

LINK A

ROLE

WT

LINK B

ROLE

WT

LINK C

ROLE

WT

INSTRUCTIONS

1. **ORIGINATING ACTIVITY:** Enter the name and address of the contractor, subcontractor, grantee, Department of Defense activity or other organization (corporate author) issuing the report.

2a. **REPORT SECURITY CLASSIFICATION:** Enter the overall security classification of the report. Indicate whether "Restricted Data" is included. Marking is to be in accordance with appropriate security regulations.

2b. **GROUP:** Automatic downgrading is specified in DoD Directive 5200.10 and Armed Forces Industrial Manual. Enter the group number. Also, when applicable, show that optional markings have been used for Group 3 and Group 4 as authorized.

3. **REPORT TITLE:** Enter the complete report title in all capital letters. Titles in all cases should be unclassified. If a meaningful title cannot be selected without classification, show title classification in all capitals in parenthesis immediately following the title.

4. **DESCRIPTIVE NOTES:** If appropriate, enter the type of report, e.g., history, progress, summary, annual, or final. Give the inclusive dates when a specific reporting period is covered.

5. **AUTHOR(S):** Enter the name(s) of author(s) as shown on or in the report. Enter last name, first name, middle initial. If unknown, show code and branch of service. The name of the principal author is an absolute minimum requirement.

6. **REPORT DATE:** Enter the date of the report as day, month, year, or month/year. If more than one date appears on the report, use date of publication.

7a. **TOTAL NUMBER OF PAGES:** The total page count should follow normal pagination procedures, i.e., enter the number of pages containing information.

7b. **NUMBER OF REFERENCES:** Enter the total number of references cited in the report.

8a. **CONTRACT OR GRANT NUMBER:** If appropriate, enter the applicable number of the contract or grant under which the report was written.

8b. **PROJECT NUMBER:** Enter the appropriate contract, department identification, such as project number, contract number, office number, task number, etc.

9. **REPORT NUMBER:** Enter the official number by which the document will be identified and controlled by the originating activity. This number must be shown in the report.

10. **REPORT NUMBER:** If the report has been assigned an official report number (either by the originator or by the sponsor), also enter this number(s).

11. **AVAILABILITY/LIMITATION NOTICES:** Enter any limitations on further dissemination of the report, other than those

imposed by security classification, using standard statements such as:

- (1) "Qualified requesters may obtain copies of this report from DDC."
- (2) "Foreign announcement and dissemination of this report by DDC is not authorized."
- (3) "U. S. Government agencies may obtain copies of this report directly from DDC. Other qualified DDC users shall request through _____."
- (4) "U. S. military agencies may obtain copies of this report directly from DDC. Other qualified users shall request through _____."
- (5) "All distribution of this report is controlled. Qualified DDC users shall request through _____."

If the report has been furnished to the Office of Technical Services, Department of Commerce, for sale to the public, indicate this fact and enter the price, if known.

11. **SUPPLEMENTARY NOTES:** Use for additional explanatory notes.

12. **SPONSORING MILITARY ACTIVITY:** Enter the name of the departmental project office or laboratory sponsoring (paying for) the research and development. Include address.

13. **ABSTRACT:** Enter an abstract giving a brief and factual summary of the document indicative of the report, even though it may also appear elsewhere in the body of the technical report. If additional space is required, a continuation sheet shall be attached.

It is highly desirable that the abstract of classified reports be unclassified. Each paragraph of the abstract shall end with an indication of the military security classification of the information in the paragraph, represented as (TS), (S), (C), or (U).

There is no limitation on the length of the abstract. However, the suggested length is from 150 to 225 words.

14. **KEY WORDS:** Key words are technically meaningful terms or short phrases that characterize a report and may be used as index entries for cataloging the report. Key words must be selected so that no security classification is required. Identifiers, such as equipment model designation, trade name, military project code name, geographic location, may be used as key words but will be followed by an indication of technical content. The assignment of links, roles, and weights is optional.

Unclassified
Security Classification